Journal of Paleontology, page 1 of 20
Copyright © The Author(s), 2023.
Published by Cambridge University Press
on behalf of The Paleontological Society
0022-3360/23/1937-2337
doi: 10.1017/jpa.2022.88

JOURNAL OF PALEONTOLOGY
A PUBLICATION OF THE Paleontological SOCIETY

Largest-known fossil penguin provides insight into the early evolution of sphenisciform body size and flipper anatomy

Daniel T. Ksepka,[1]* Daniel J. Field,[2,3] Tracy A. Heath,[4] Walker Pett,[4] Daniel B. Thomas,[5] Simone Giovanardi,[5] and Alan J.D. Tennyson[6]

[1]Bruce Museum, Greenwich, CT, USA <dksepka@brucemuseum.org>
[2]Department of Earth Sciences, University of Cambridge, Cambridge, CB2 3EQ, UK
[3]Museum of Zoology, University of Cambridge, Cambridge, CB2 3EJ, UK <djf70@cam.ac.uk>
[4]Department of Ecology, Evolution and Organismal Biology, Iowa State University, Ames, IA 50011, USA <phylo@iastate.edu> <will.pett@gmail.com>
[5]School of Natural Sciences, Massey University, Auckland, 0632 New Zealand, <d.b.thomas@massey.ac.nz> <giovanerd90@gmail.com>
[6]Museum of New Zealand Te Papa Tongarewa, PO Box 467, Wellington, New Zealand <alant@tepapa.govt.nz>

Abstract.—Recent fossil discoveries from New Zealand have revealed a remarkably diverse assemblage of Paleocene stem group penguins. Here, we add to this growing record by describing nine new penguin specimens from the late Paleocene (upper Teurian local stage; 55.5–59.5 Ma) Moeraki Formation of the South Island, New Zealand. The largest specimen is assigned to a new species, *Kumimanu fordycei* n. sp., which may have been the largest penguin ever to have lived. Allometric regressions based on humerus length and humerus proximal width of extant penguins yield mean estimates of a live body mass in the range of 148.0 kg (95% CI: 132.5 kg–165.3 kg) and 159.7 kg (95% CI: 142.6 kg–178.8 kg), respectively, for *Kumimanu fordycei*. A second new species, *Petradyptes stonehousei* n. gen. n. sp., is represented by five specimens and was slightly larger than the extant emperor penguin *Aptenodytes forsteri*. Two small humeri represent an additional smaller unnamed penguin species. Parsimony and Bayesian phylogenetic analyses recover *Kumimanu* and *Petradyptes* crownward of the early Paleocene mainland NZ taxa *Waimanu* and *Muriwaimanu*, but stemward of the Chatham Island taxon *Kupoupou*. These analyses differ, however, in the placement of these two taxa relative to *Sequiwaimanu*, *Crossvallia*, and *Kaiika*. The massive size and placement of *Kumimanu fordycei* close to the root of the penguin tree provide additional support for a scenario in which penguins reached the upper limit of sphenisciform body size very early in their evolutionary history, while still retaining numerous plesiomorphic features of the flipper.

UUID: https://zoobank.org/15b1d5b2-a5a0-4aa5-ba0a-8ef3b8461730

Introduction

Zealandia is a center of extant penguin diversity, and accumulating fossil evidence supports the hypotheses that both total-group and crown penguins originated in this region (Thomas et al., 2020b). The oldest and most stemward-known fossil penguin, *Waimanu manneringi* Ando, Jones, and Fordyce in Slack et al., 2006, was uncovered in the early Paleocene (ca. 61.6–60.5 Ma) Waipara Greensand of the South Island of New Zealand (Slack et al., 2006). Since that discovery, a number of additional stem group penguins have been reported from the Waipara Greensand, capturing the morphology of penguins during the early stages of the evolution of flightless wing-propelled diving (Mayr et al., 2017a, b, 2019). Contemporary penguin fossils from the Paleocene Takatika Grit (62.5–60 Ma) have been reported from the Chatham Islands, an archipelago located ~750 km from mainland New Zealand (Blokland et al., 2019). Slightly younger penguins from the late Paleocene Moeraki Formation (59.5–55.9 Ma) occur on mainland New Zealand. Two Moeraki Formation penguin specimens have been published to date: a partial coracoid and scapula of a modest-sized penguin mentioned briefly in a review (Fordyce and Jones, 1990) and a partial skeleton of the giant stem penguin *Kumimanu biceae* Mayr et al., 2017a. A crushed distal end of a tibiotarsus (OU8743) from the Moeraki Formation, which was identified as belonging to a large bird by Fordyce (1991), also appears to belong to a penguin (A.J.D.T., personal observation, 2015).

Along with the aforementioned Paleocene fossils, younger specimens ranging in age from the early Eocene *Kaiika maxwelli* Fordyce and Thomas, 2011 (Kauru Formation), to the recently extinct *Eudyptes warhami* Cole et al., 2019, document a remarkable diversity of 23 named penguin species from the fossil record of New Zealand, with additional taxa either awaiting formal description or inferred to be present based on fragmentary material (Huxley, 1859; Oliver, 1930; Marples, 1952, 1960; Simpson, 1971, 1972; Fordyce and Thomas, 2011; Ksepka et al., 2012; Thomas and Ksepka, 2016; Mayr et al.,

*Corresponding author.

https://doi.org/10.1017/jpa.2022.88 Published online by Cambridge University Press

2017a, b; Cole et al., 2019; Thomas et al., 2020a, b; Giovanardi et al., 2021).

One surprising insight into the evolutionary history of penguins revealed by recent discoveries is the apparently rapid attainment of enormous body size in the Paleocene, as evinced by specimens with proportions greatly outstripping those of the largest extant penguins (Tambussi et al., 2005; Mayr et al., 2017b). Given that the earliest giant New Zealand penguin fossils pre-date the occurrence of penguins on other continents, it is tempting to speculate that penguins approached the peak of their known body size distribution while still restricted to their Zealandian center of origin. However, this hypothesis remains largely untested due to gaps in the early Paleocene marine record elsewhere in the Southern Hemisphere, and uncertainties regarding the phylogenetic relationships among early stem penguins. Therefore, untangling the phylogenetic relationships of Paleocene stem penguins has potential to clarify key aspects of penguin macroevolutionary change. These include revealing the tempo and pattern of sphenisciform body size evolution and providing new insight into the evolution of the characteristic penguin bauplan, including their distinctive flipper apparatus.

In this study, we report nine new stem penguin specimens from the late Paleocene Moeraki Formation. All were collected from beach-washed boulders at Hampden Beach (Otago, New Zealand) (Fig. 1). At this locality, concretions occur in situ in mudstones but are more often found completely exhumed from the softer surrounding matrix by coastal erosion (A.J.D.T., personal observation, 2021). The new penguin specimens were all found within the intertidal zone in remnants of concretions that had been shattered by the elements to reveal their interiors. Given the state of wear and rounding of many of these rocks, most evidently had been subject to wave action for many years. Although this leaves their precise stratigraphic horizon uncertain, the contact between the Moeraki Formation and the overlying Kurinui Formation is considered to be equivalent to the Teurian/Waipawan boundary (and hence the Paleocene/Eocene boundary) (Morgans, 2009), providing a minimum age of ca. 56.0 Ma for the fossils. The upper part of the Moeraki Formation exposed at Hampden Beach is specifically considered to represent the upper Teurian local stage based on evidence from microfossils (Crouch and Brinkhuis, 2005; Morgans, 2009). Evidence from agglutinated foraminiferal taxa suggests that the fossiliferous concretions originally formed in a relatively shallow shelf to upper bathyal environment (Morgans, 2009).

The largest of the new fossils belongs to a new species of giant penguin represented by a partial associated skeleton, including the largest penguin humerus yet reported. An additional large fossil can be referred to cf. *Kumimanu biceae*, and five smaller specimens belong to a penguin slightly larger than the extant emperor penguin, *Aptenodytes forsteri* Gray, 1844, that we describe as a second new species. The two smallest specimens belong to an unnamed penguin intermediate in size between the king penguin *Aptenodytes patagonicus* Miller, 1778, and the emperor penguin. We provide allometric regressions based on the dimensions of humeri from crown penguins to estimate body mass in the new fossil taxa and present an expanded phylogeny of extinct and extant total clade penguins.

Materials and methods

Anatomical nomenclature.—In the descriptions below, we use the anatomical terminology of Baumel and Witmer (1993). Following the recent suggestion of Richards (2019), who considered that the vertical posture of penguins results in the terms "cranial" and "caudal" being applied to different faces of the flipper than when applied to the wings of a typical bird, we orient the humerus in an "extended during swimming" position for purposes of the description (e.g., the oblong fossa marking the insertion of m. pectoralis is placed on the ventral face of the bone in this context).

3D digital replicas.—Digital replicas of fossils (i.e., 3D meshes) were generated using a HandySCAN BLACK handheld laser scanner (Creaform Inc., Quebec, Canada). 3D scan data were processed using VXelements 9.1.0 (Creaform Inc., Quebec, Canada). To facilitate systematic comparisons, humeri were digitally extracted from their respective fossil blocks and made into watertight meshes using VXelements 9.1.0. 3D meshes were rendered using Blender 2.93 (Blender Online Community, 2022) and were digitally mirrored when necessary to facilitate comparisons between left versus right elements. The minimum resolvable surface feature of the 3D models was ~0.2 mm diameter.

The humerus of NMNZ S.47426 has been twisted out of life position by deformation. In order to correct this distortion, we used Blender 2.93 to digitally separate the head from the diaphysis, and then to separate the head into two sections, with the separation following the broken edges between each part. We then manually reoriented these three parts using digital models of other fossil penguin humeri as visual guides.

Phylogenetic analyses.—We scored the new species into a data set based on the extant penguin matrix of Bertelli and Giannini (2005), which was expanded to include fossil taxa by Ksepka et al. (2006) and has been modified and expanded in numerous subsequent studies, most recently by Giovanardi et al. (2021). We added the previously described fossil penguins *Crossvallia unienwillia* Tambussi et al., 2005, *Crossvallia waiparensis* Mayr et al., 2019, *Kaiika maxwelli*, and *Kupoupou stilwelli* Blokland et al., 2019, and added or modified seven characters to represent new features observed in our review of recently collected Paleocene penguin material. The expanded matrix comprises 279 morphological characters and 2 outgroups, 20 extant penguin taxa, and 44 fossil penguin taxa.

Phylogenetic analyses were conducted using PAUP*4.0a168 (Swofford, 2003) with a heuristic search strategy specifying 10,000 replicates of random taxon addition holding 10 trees per replicate, with TBR branch swapping limited to 10,000,000 rearrangements per replicate. All characters were equally weighted, multistate codings were considered to represent polymorphism, and branches with a minimum length of zero were collapsed.

Bayesian phylogenetic analysis was conducted using RevBayes 1.1.1 (Höhna et al., 2016) using a specimen-level

https://doi.org/10.1017/jpa.2022.88 Published online by Cambridge University Press

fossilized birth-death process as the prior on the tree topology and divergence times (Stadler, 2010; Heath et al., 2014), with exponential hyperpriors on the diversification parameters. These analyses follow the protocol found in the RevBayes tutorial (https://revbayes.github.io/tutorials/fbd/fbd_specimen.html). Two chains were run with 1 move per generation until the maximum difference of clade frequencies (max_diff, Lartillot and Philippe, 2004) was <0.1 (350,000,000 generations). All data and scripts associated with these analyses are provided in the supplementary information.

Repositories and institutional abbreviations.—AMNH, Department of Ornithology, American Museum of Natural History, New York, U.S.A.; CM, Canterbury Museum, Christchurch, New Zealand; IB/P/B, Institute of Biology, University of Białystok, Białystok, Poland; MEF, Museo Egidio Feruglio, Trelew, Argentina; MLP, Museo de La Plata, La Plata, Argentina; NMNZ, Museum of New Zealand Te Papa Tongarewa, Wellington, New Zealand; MUSM, Museum of San Marcos University, Lima, Peru; MNHN, Muséum National d'Histoire Naturelle, Paris, France; OM, Otago Museum, Dunedin, New Zealand; OU, Geology Museum, University of Otago, Dunedin, New Zealand; SAM, Iziko South African Museum, Cape Town, South Africa; SGO-PV, Sección de Paleontología del Museo Nacional de Historia Natural, Santiago, Chile; UCMP, University of California Museum of Paleontology, Berkeley, California, U.S.A.; UCN, Museo Geológico Prof. Humerto Fuenzalida, Universidad Católica del Norte; WM, Waikato Museum, Hamilton, New Zealand.

Systematic paleontology

Aves Linnaeus, 1758
Sphenisciformes Sharpe, 1891
Kumimanu Mayr, Scofield, De Pietri, and Tennyson 2017

Type species.—*Kumimanu biceae* Mayr, Scofield, De Pietri, and Tennyson 2017.

Revised diagnosis.—Differs from all other Paleocene penguins in larger size and in robust femur shaft (observable only in *Kumimanu biceae*). Differs from *Waimanu*, *Muriwaimanu* Mayr et al., 2017b, *Sequiwaimanu* Mayr et al., 2017b, and *Petradyptes* n. gen. in lacking ovoid depressions on the lateral faces of the posterior thoracic vertebrae. Differs from *Muriwaimanu*, *Sequiwaimanu*, and *Kupoupou* in impressio m. pectoralis forming an extremely wide fossa. Differs from *Waimanu*, *Muriwaimanu*, *Sequiwaimanu*, and *Crossvallia* in greater distal extension of insertion scar for m. supracoracoideus (condition unknown in *Waimanu*) and placement of sulcus extensorius of tibiotarsus close to midline. Differs from *Kaiika* and *Petradyptes* in less strongly flattened humeral shaft. Further differs from all post-Paleocene penguins other than *Kaiika* in having the border of the sulcus scapulotricipitalis formed by a short posterior trochlear ridge, positioned on the ventral face of the humerus (versus a longer posterior trochlear ridge extending to the caudal border of the humeral shaft in Eocene and later penguins).

Kumimanu fordycei new species
Figure 2

Holotype.—NMNZ S.47426: complete cervical vertebra, partial right coracoid, partial right scapula, nearly complete right humerus, shaft of right ulna, tentatively identified left and right patellae, fragment of left tibiotarsus, and several unidentified fragments of bone. Measurements in Table 1.

Diagnosis.—Differs from *Kumimanu biceae* by substantially larger size (humerus midshaft width 40.7 mm versus 33.0 mm), more curved humerus shaft, and proportionally less expanded proximal end (proximal width ≈ 2.0 times midshaft width versus 2.27 times midshaft width in *Kumimanu biceae*).

Occurrence.—The holotype was collected in a beach-washed concretion from the Moeraki Formation at Hampden Beach, North Otago, New Zealand (Fig. 1). This site is cataloged under NZ Fossil Record Number J42/f0956 (precise locality information is recorded at NMNZ).

Description.—The holotype is preserved in a concretion (Fig. 2). The humerus, coracoid, and scapula are nearly in contact at the shoulder joint, whereas the remaining elements are disarticulated and scattered throughout the block. A single vertebra appears to correspond to cervical vertebra 5. It is heterocoelous and bears a short processus spinosus, a completely enclosed foramen transversarium, and a well-developed processus transversus. The articular facets of the zygapophysis cranialis and zygapophysis caudalis are extremely enlarged compared to those of extant penguins (Fig. 2.3). Enlarged facets on the vertebral articular processes are observed in other giant stem penguins such as *Icadyptes salasi* Clarke et al., 2007, whereas the proportions of these facets in smaller-bodied Paleocene penguins like *Sequiwaimanu rosieae* Mayr et al., 2017b, resemble those of crown penguins (Ksepka et al., 2008).

The right scapula is preserved in two segments: a portion of the omal end and a larger portion of the blade. The tuberculum coracoideum is strongly rounded and omally projected. The ball-like morphology of the tuberculum coracoideum is very similar to that in *Kumimanu biceae*, although it is clearly larger in absolute size. In the smaller Paleocene stem penguins *Muriwaimanu tuatahi* (Ando, Jones, and Fordyce in Slack et al., 2006) and *Sequiwaimanu rosieae*, the tuberculum coracoideum is also rounded, but is proportionally smaller and more weakly projected. A more oblong shape characterizes the tuberculum coracoideum in later stem penguins such as *Icadyptes salasi*, as well as extant penguins. Unfortunately, the acromion and facies articularis humeralis are not preserved. The intact portion of the scapular blade indicates it was flattened and widened but lacked the paddle-like distal expansion seen in Neogene penguins. Compared to *Kumimanu biceae*, the scapular blade of the new species appears less expanded, but this is possibly an artifact of preservation because the borders of the blade are slightly eroded.

The coracoid is nearly complete except for the omal end, but is generally poorly preserved. The length from the facies articularis sternalis to the omal rim of the cotyla scapularis is ~176 mm. If the proportions of the missing omal tip were similar to those in *Sequiwaimanu rosieae*, the coracoid would have been slightly shorter than the humerus, as in other Paleogene penguins. Such proportions would represent an intermediate condition

https://doi.org/10.1017/jpa.2022.88 Published online by Cambridge University Press

Table 1. Measurements from Moeraki Formation penguin fossils. All measurements in mm.

Taxon	Specimen	Element	Dimension	Measurement (mm)
Kumimanu fordycei n. sp. holotype	NMNZ S.47426	cervical vertebra 5	minimum height, facies articularis caudalis	20.3
			maximum height, facies articularis caudalis	23.7
			minimum width, facies articularis caudalis	23.7
			maximum width, facies articularis caudalis	27.2
			width, articular face, zygopophysis cranialis	61.5
			width, articular face, zygopophysis caudalis	57.5
		humerus	maximum length as preserved	236.0
			estimated complete length	~243
			length from head to condylus ventralis as preserved	230.0
			estimated length from head to condylus ventralis	~237
			maximum proximal width	~83.5
			midshaft width	40.7
			midshaft depth	21.5
cf. *Kumimanu biceae*	NMNZ S.47931	femur	length as preserved	137.0
			estimated length	~150–160
			width, proximal end	45
Petradyptes stonehousei n. gen. n. sp. holotype	NMNZ S.47114	humerus	maximum length as preserved	139.0
			estimated complete length	~152
			length from head to condylus ventralis as preserved	136.0
			estimated length from head to condylus ventralis	~140
			maximum proximal width	53.4
			midshaft width	30.4
			midshaft depth	~12.0
cf. *Petradyptes stonehousei* n. gen. n. sp.	NMNZ S.47933	humerus	maximum proximal width	~55.0
cf. *Petradyptes stonehousei* n. gen. n. sp.	NMNZ S.47146	femur	length	~131.0
			midshaft width	15.6
cf. *Petradyptes stonehousei* n. gen. n. sp.	NMNZ S.47927	carpometacarpus	distal width	~20.0
cf. *Petradyptes stonehousei* n. gen. n. sp.	NMNZ S.46081	carpometacarpus	length to distal margin of metacarpal II	70.8
			length to distal margin of metacarpal III	73.3
			distal width	21.1
		femur	proximal width	36.0
			length	~125.0
			midshaft width	15.2

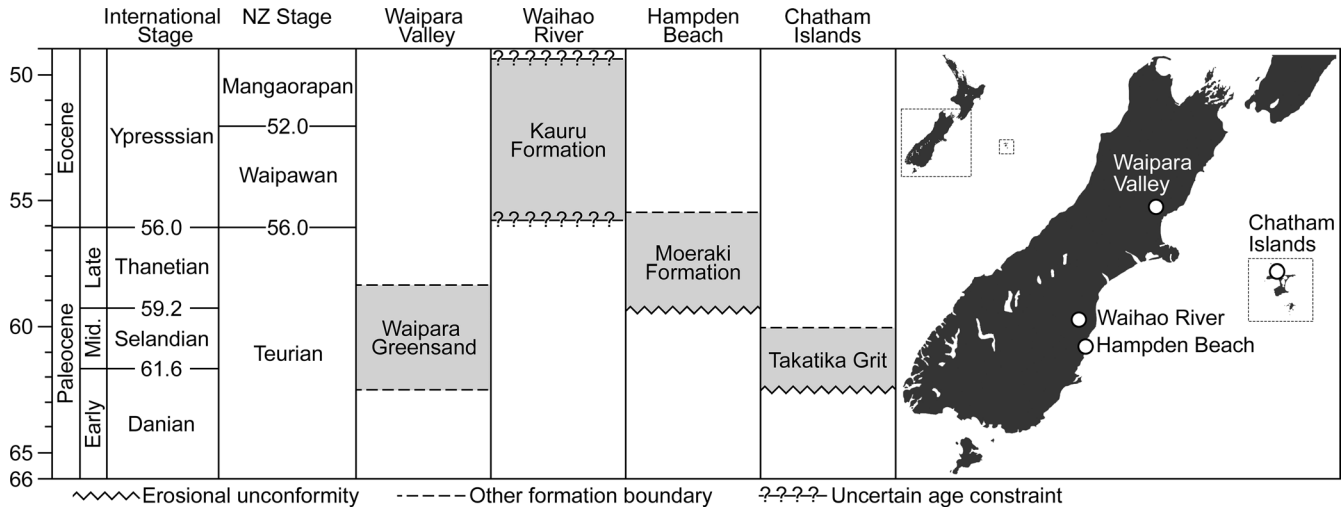

Figure 1. Simplified comparison of stratigraphic horizons for key Paleogene penguin localities in New Zealand. Fossil sites discussed in this paper are indicated on map at right.

between volant birds and later penguins: the coracoid is much shorter than the humerus in most extant birds, whereas the coracoid exceeds the humerus in length in all known Eocene and later penguins. The facies articularis sternalis is greatly widened and the presence of a processus lateralis cannot be determined.

The humerus is nearly complete, lacking only the distal condyles, although some morphological features are obscured by erosion or overlying bones and the proximal part of the caput humeri has been damaged. The shaft is strongly flattened and tapers distally. The impressio m. pectoralis forms an extremely wide fossa (Fig. 2.4), closely resembling the condition in *Kaiika maxwelli* and, to a lesser extent, some Alcidae. This oblong impression extends far distal to the level of the crista bicipitalis. The distal margins of the impressio m. pectoralis and crista bicipitalis appear to be at the same level in *Kumimanu biceae* (Fig. 3), however this may be at

https://doi.org/10.1017/jpa.2022.88 Published online by Cambridge University Press

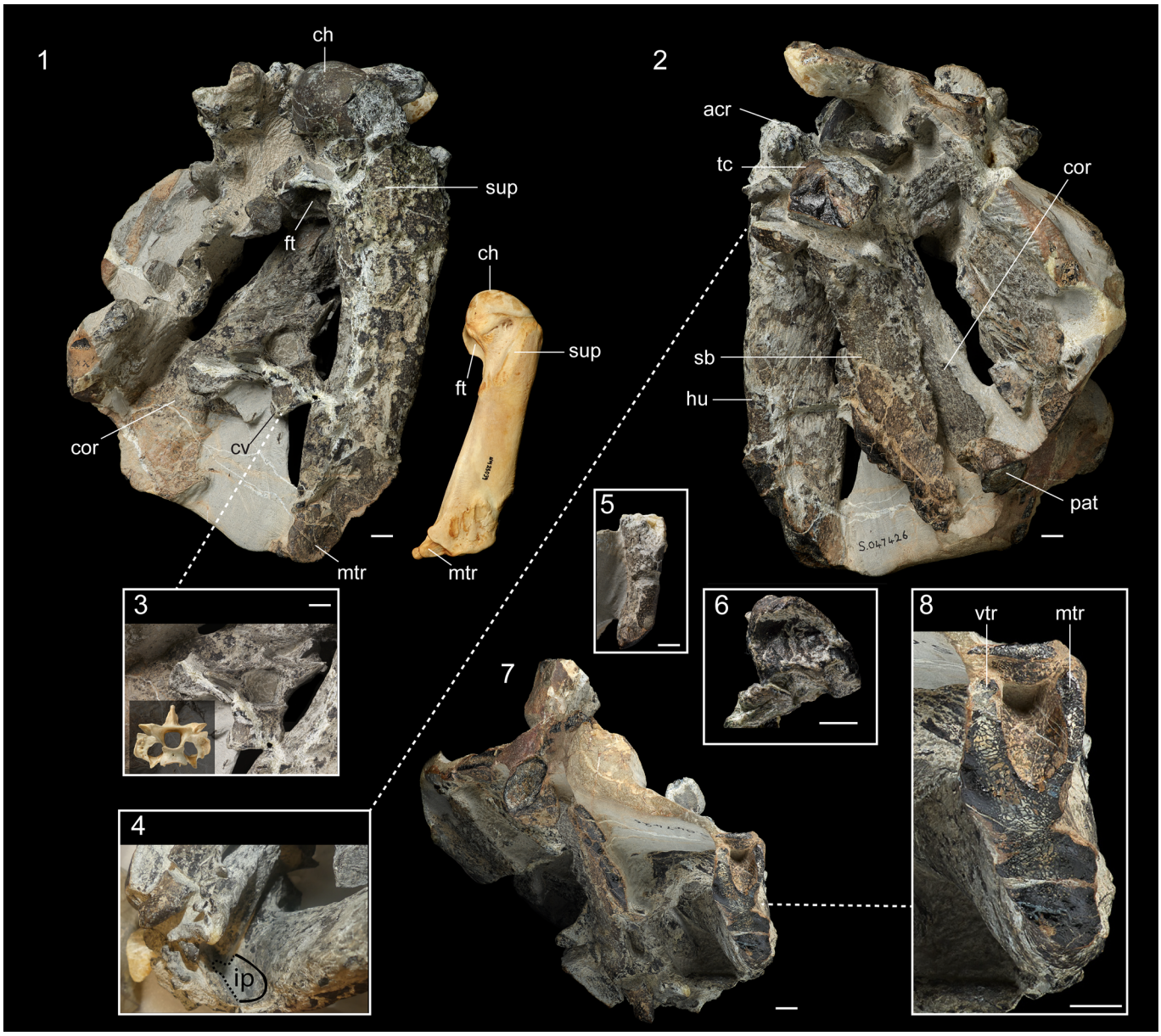

Figure 2. *Kumimanu fordycei* n. sp. holotype (NMNZ S.47426). (**1**) Holotype block oriented to show humerus in dorsal view with humerus of an extant emperor penguin (*Aptenodytes forsteri*; NMNZ OR.23039) oriented in the same view to indicate scale, (**2**) block oriented with humerus in ventral view (partially overlain by scapula), (**3**) comparison of fifth cervical vertebra in caudal view with fifth cervical vertebra of emperor penguin for scale, (**4**) oblique view of humerus showing wide fossa formed by impressio m. pectoralis (which is partially hidden by overlying elements) in ventral view. (**5**) Distal portion of ulna shaft in dorsal view. (**6**) Close-up of tentatively identified patella. (**7**) Block oriented with distal end of humerus exposed and (**8**) close up of distal trochlea. Abbreviations: **acr**, processus acrocoracoideus; **ch**, caput humeri; **cor**, coracoid; **cv**, cervical vertebral; **ft**, fossa tricipitalis; **hu**, humerus; **ip**, impressio m. pectoralis; **mtr**, middle trochlear ridge; **pat**, patella; **sb**; scapular blade; **sup**, insertion scar for m. supracoracoideus; **tc**, tuberculum coracoideum, **vtr**, ventral trochlear ridge. Scale bars equal 10 mm.

least in part an artifact of preparation given that the matrix has not been completely removed from the impression. The m. supracoracoideus insertion scar is elongated, raised, and shifted towards the caudal border of the shaft. The fossa tricipitalis is very deep and appears to have been undivided, although matrix obscures its exact dimensions. The ventral and middle trochlear ridges are intact, whereas the dorsal trochlear ridge has been lost to erosion (Fig. 2.8). The ventral and middle trochlear ridges are much more deeply separated than in crown penguins. The absence of the dorsal trochlear ridge indicates that it must have been anteriorly placed and failed to extend to the level of the other two trochleae, as in other Paleocene penguins.

A portion of the right ulna including the distal third of the shaft is preserved, although the distal articular region is lost. The cross-section is ovoid, as in *Kumimanu biceae*, being less dorsoventrally flattened than in post-Paleocene penguins.

Two small irregular elements are tentatively identified as patellae. Each is block-like and has one strongly rimmed concave face resembling the articular surface for the femur; the more complete of the two also preserves a second concave face corresponding to the articular surface for the tibiotarsus

https://doi.org/10.1017/jpa.2022.88 Published online by Cambridge University Press

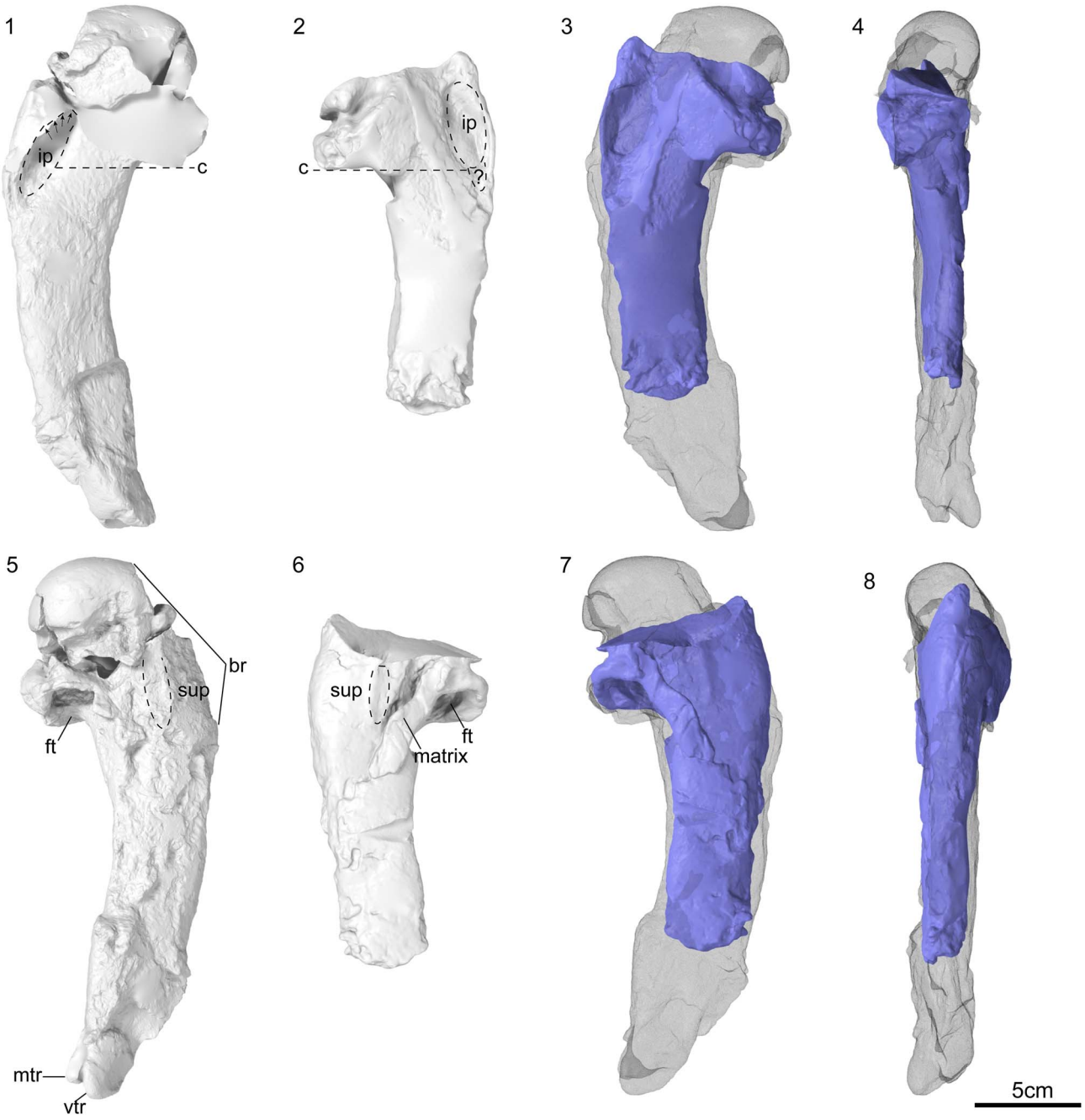

Figure 3. Comparison of the digitally reconstructed holotype humerus of *Kumimanu biceae* (NMNZ S.45877) and the holotype humerus of *Kumimanu fordycei* n. sp. (NMNZ S.47426). Images show watertight models after digital extraction from fossil blocks, rendered using Blender 2.93 (Blender Online Community, 2022). The two broken sections of the head were digitally re-aligned to one another and to the diaphysis for *Kumimanu fordycei*. Ventral view of (**1**) right humerus from *K. fordycei* n. sp. and (**2**) left humerus of *K. biceae*. (**3, 4**) Digitally mirrored *K. biceae* humerus (blue) overlain on *K. fordycei* humerus (wireframe) in (**3**) ventral and (**4**) caudal view. Dorsal view of (**5**) right humerus from *K. fordycei* and (**6**) left humerus of *K. biceae*. (**7, 8**) Digitally mirrored *K. biceae* humerus (blue) overlain on *K. fordycei* humerus (wireframe) in (**7**) dorsal and (**8**) cranial view. Abbreviations: **br**, broken margin; **c**, line indicating level of distal margin of crista bicipitalis; **ft**, fossa tricipitalis; **ip**, impressio m. pectoralis; **matrix** = matrix/bone fragment adhering to surface of humerus; **mtr**, middle trochlear ridge; **sup**, insertion scar for m. supracoracoideus; **vtr**, ventral trochlear ridge; **?**, possible extension of impressio m. pectoralis obscured by matrix. Arrows indicate extension of impressio m. pectoralis, which is obscured by overlying matrix in NMNZ S.47426.

(Fig. 2.6). Provided our identification of these ossifications as patellae is correct, they are smaller relative to body size than those of extant penguins (the long axis is within the size range of the much smaller emperor penguin). Unlike extant penguins, these elements also lack a sulcus or canal for the tendon of m. ambiens.

A small fragment of the left tibiotarsus, comprising the rim of the condylus medialis, is preserved near the head of the humerus at the edge of the block and was separated during preparation. As is typical for penguins, the epicondylus medialis is strongly developed. Its distal rim appears to lack the pronounced notch that is characteristic of Procellariiformes (the

https://doi.org/10.1017/jpa.2022.88 Published online by Cambridge University Press

extant sister group to penguins), but which is extremely weakly developed or absent in most penguins. The mediolateral width of the condylus medialis is proportionally narrower than in extant penguins.

Etymology.—In honor of R. Ewan Fordyce, in recognition of his contributions to the field of paleontology including his discovery, collection, and study of penguin fossils in New Zealand and Antarctica, and his generous mentorship of many paleontologists, including authors DTK and DBT, throughout their careers.

Remarks.—*Kumimanu fordycei* is a candidate for the largest known penguin, as discussed below.

cf. *Kumimanu biceae*
Figure 4

Holotype.—NMNZ S.45877: associated partial skeleton including three vertebrae and partial synsacrum, partial left scapula and right coracoid, cranial section of sternum, partial left humerus and ulna, right femur, and partial right tibiotarsus.

Occurrence.—Late Paleocene Moeraki Formation at Hampden Beach, North Otago, New Zealand.

Description.—The neck of the right femur is very thick, such that there is little constriction between the head and the shaft. The shaft of the left femur is unfortunately partially lost, thus a midshaft diameter cannot be reliably obtained. Based on the intact portion, we estimate this bone was slightly shorter than the femur of the *Kumimanu biceae* holotype. The proximal ends of the tibiotarsus and fibula, which are not preserved in any other specimens of *Kumimanu*, are intact. The crista cnemialis lateralis is relatively thin and comes to a sharp point. In caudal view, the ridge running along the long axis of the shaft is more prominent than in extant penguins.

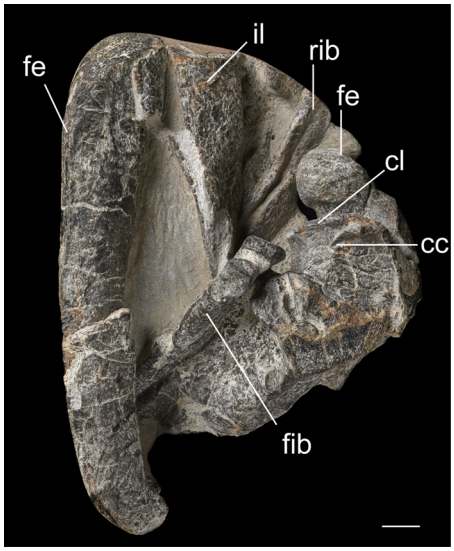

Figure 4. cf. *Kumimanu biceae* (NMNZ S.47931) proximal end of right femur and shaft of left femur, proximal ends of left tibiotarsus and fibula. Abbreviations: **cc**, crista cnemialis cranialis; **cl**, crista cnemialis lateralis; **fe**, femur; **fib**, fibula, **il**, tentatively identified iliac blade fragment; **rib**, rib. Scale bar equals 10 mm.

Materials.—NMNZ S.47931: fragments of rib and ilium, proximal end of right femur and shaft of left femur, proximal ends of left tibiotarsus and fibula. Measurements in Table 1.

Remarks.—The referred specimen also belongs to a giant penguin, but is too small to belong to *Kumimanu fordycei*. The proximal end of the right femur is 45 mm wide versus 52 mm in the holotype of *Kumimanu biceae*, suggesting it may belong to a smaller individual of that species. Intraspecific size variation in stem penguins remains poorly understood, but the referred leg bones provide additional support for recognition of two species of *Kumimanu* because the holotype specimen of *K. fordycei* represents an individual ~15% larger than that represented by the holotype specimen of *K. biceae*, which in turn represents an individual ~15% larger than NMNZ S.47931.

Petradyptes new genus

Type species.—*Petradyptes stonehousei* n. gen. n. sp.

Diagnosis.—As for the type species by monotypy.

Etymology.—From the Greek *petra* for rock and *dyptes* for diver. In Ancient Greek, *petra* carries a connotation of rock cliffs by the sea, eliciting the fossil locality.

Remarks.—Although not the most complete of the specimens, we selected NMNZ S.47114 as the holotype to ease comparisons with existing Paleocene penguin species, the majority of which are based on holotypes that include a humerus. Several additional specimens are also assigned to *Petradyptes*. NMNZ S.47933 also preserves the proximal end of the humerus, which agrees well in size and morphology with the holotype and preserves the proximal end of the tibiotarsus, which in turn agrees well with the proximal tibiotarsus of NMNZ S.46081. NMNZ S.46081 preserves the femur and carpometacarpus, allowing comparisons to NMNZ S.47146 and NMNZ S.47927. This chain of evidence and the consistent overall size of the specimens support the conclusion that all belong to *Petradyptes*, although we consider these referrals provisional pending discovery of more complete specimens preserving the humerus.

Petradyptes stonehousei new species
Figures 5, 6

Holotype.—NMNZ S.47114: nearly complete right humerus and distal portion of left femur. Measurements in Table 1.

Diagnosis.—Differs from all other Paleocene penguins in strongly flattened humerus shaft (midshaft width more than twice midshaft depth). Differs from *Muriwaimanu*, *Sequiwaimanu*, and *Kupoupou* in wider fossa formed by impressio m. pectoralis. Differs from *Muriwaimanu*, *Sequiwaimanu*, and *Crossvallia* in more distally extended

https://doi.org/10.1017/jpa.2022.88 Published online by Cambridge University Press

Figure 5. *Petradyptes stonehousei* n. gen. n. sp. holotype (NMNZ S.47114) complete right humerus and distal portion of left femur in (**1**) ventral view and (**2**) dorsal view. Abbreviations: **cb**, insertion scar for m. coracobrachialis caudalis; **cc**, insertion scar for m. coracobrachialis caudalis; **fe**, femur shaft; **ft**, fossa tricipitalis; **ip**, impressio m. pectoralis; **ftd**, fossa tricipitalis dorsalis; **sup**, insertion scar for m. supracoracoideus. Scale bar equals 10 mm.

insertion scar for m. supracoracoideus. Differs from *Kaiika* in proportionally wider humerus shaft, greater proximodistal length of crista bicipitalis, and more proximodistally elongate scar for m. supracoracoideus. We note that the deep groove on the tuberculum ventrale of *Kaiika maxwelli*, which was originally considered autapomorphic for that species, is more likely to be an artifact of incomplete preservation of the natural mold used to cast the holotype humerus.

Occurrence.—Late Paleocene Moeraki Formation, Hampden Beach, North Otago, New Zealand.

Description.—The holotype humerus is strongly sigmoid in shape (Fig. 5). It is only slightly longer (estimated complete length 150 mm) than the humerus of *Kaiika maxwelli* (146.8 mm), but the shaft is ~50% wider and is more strongly dorsoventrally flattened. As in *Kumimanu* and *Kaiika*, the fossa formed by impressio m. pectoralis is extremely wide. It is deep near its proximal end, becoming shallower distally. The m. supracoracoideus insertion scar is strongly raised, although less so than in earlier Paleocene taxa such as *Muriwaimanu* and *Sequiwaimanu*. The scar extends distally to the level of the rim of the fossa tricipitalis and is positioned close to the midline of the shaft as in *Muriwaimanu* and *Sequiwaimanu*, whereas it is shifted towards the caudal border of the shaft in *Kumimanu* and most other penguins. The distal margin of the crista bicipitalis forms a convex projection, which resembles that of *Muriwaimanu tuatahi* and *Kaiika maxwelli*. The insertion scar for m. coracobrachialis caudalis is short and ovoid, oriented almost craniolaterally, and clearly separated from the head. In turn, a platform of bone proximal to the scar separates the incisura capitis from the fossa tricipitalis dorsalis, which is deep, but occupies a small area due to being impinged upon by the m. supracoracoideus insertion scar. The distal end, including the condyles and trochlear processes, is missing.

NMNZ S.46081 (Fig. 6.1–6.5) is the most informative referred specimen. The intact portion of the sternum measures 177 mm, but it is unfortunately lacking both its cranial and caudal margins. Because no indication of the incisura caudalis is visible along the lateral margin, the sternum must have been considerably longer when complete. A prominent intramuscular line is developed. This feature varies in prominence in extant

https://doi.org/10.1017/jpa.2022.88 Published online by Cambridge University Press

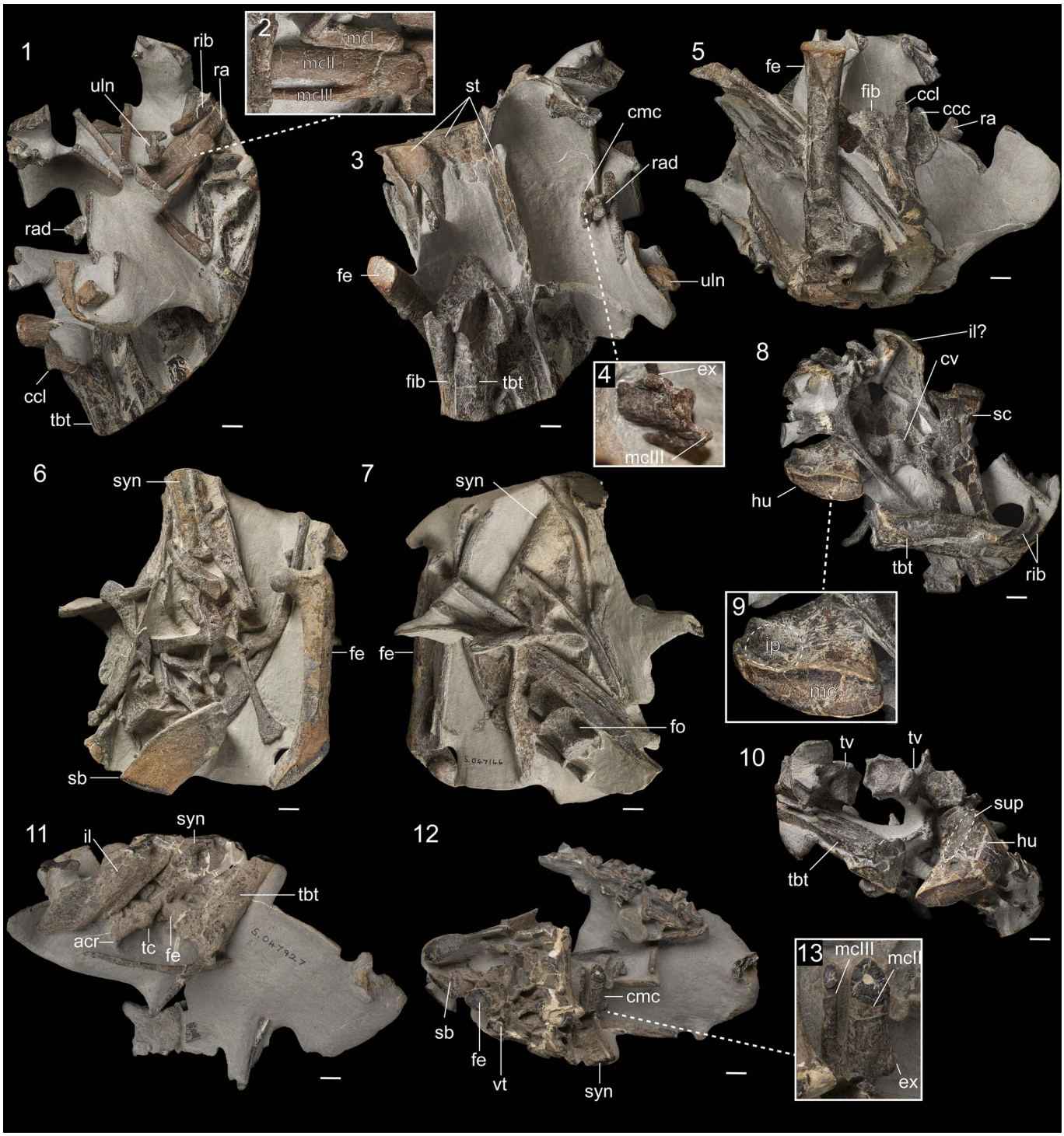

Figure 6. Referred specimens of *Petradyptes stonehousei*. (**1-5**) NMNZ S.46081, oriented (**1**) exposing carpometacarpus in dorsal view with (**2**) close up of proximal portion of carpometacarpus, (**3**) exposing proximal end of tibiotarsus in cranial view with (**4**) close up of distal end of carpometacarpus, and (**5**) exposing femur in caudal view. (**6-7**) NMNZ S.47146, oriented (**6**) exposing femur in cranial view and pelvis in dorsal view and (**7**) exposing femur in caudal view and synsacrum in ventral view. (**8-10**) NMNZ S. 47933, oriented (**8**) with humerus exposed in oblique view showing dorsal face of proximal end and cross-section of broken shaft with (**9**) close-up showing wide fossa pectoralis, and (**10**) exposing proximal end of humerus in dorsal view. (**11-13**) NMNZ S. 47927 oriented (**11**) exposing omal end of scapula and distal end of tibiotarsus and (**12**) exposing broken carpometacarpus with (**13**) close up of distal end of carpometacarpus with exposed cross-section near midshaft. Abbreviations: **acr**, acromion; **ccc**, crista cnemialis cranialis; **ccl**, crista cnemialis lateralis; **cmc**, carpometacarpus; **cv**, cervical vertebra; **ex**, expansion at distal end of metacarpal II; **fe**: femur; **fib**, fibula; **fo**, fossa; **fp**, fossa pectoralis; **hu**, humerus; **il**, iliac blade; **ip**, impressio m. pectoralis; **mc**, medullary cavity; **mcI**, alular metacarpal; **mcII**, metacarpal II; **mcIII**, = metacarpal III; **ra**, radius; **rad**, radiale; **rib**, rib; **sb**, scapular blade; **sc**, scapula; **st**, sternum; **sup**, insertion scar for m. supracoracoideus, **syn**, synsacrum; **tbt**, tibiotarsus; **tc** tuberculum coracoideum; **tv**, thoracic vertebra; **uln**, ulnare, **vt**, vertebra (position uncertain). Scale bars equal 10 mm.

https://doi.org/10.1017/jpa.2022.88 Published online by Cambridge University Press

penguins. Based on the intact left side near mid-keel, the sternum width would have been within the range of the extant emperor penguin despite its greater length. These proportions together suggest an elongate and slender sternum, resembling that of *Kairuku* in general proportions (see Ksepka et al., 2012, fig. 3).

The radiale is more robust and mediolaterally wider than in extant penguins. The ulnare is greatly expanded, but has a disc-like shape, unlike the sharp triangular shape present in crown penguins. The carpometacarpus is slightly shorter than the species average for emperor penguins. Complete skeletons of Paleocene penguins are rare, but the wing proportions in associated skeletons of *Muriwaimanu* and *Sequiwamanu* indicate that the carpometacarpus was proportionally shorter relative to the humerus, as in other early stem penguins. Based on the proportions of *Muriwaimanu* and *Sequiwamanu*, the carpometacarpus length of NMNZ S.46081 (proximal margin to distal margin of metacarpal II: 70.8 mm) falls within the size expected for *Petradyptes stonehousei* based on humerus length in the holotype (predicted range 68.5–74.4 mm). The proximal end of the carpometacarpus is partially embedded in matrix and is exposed in dorsal view (Fig 6.2), whereas the distal end of the carpometacarpus projects free from the matrix (Fig. 6.4). As in other Paleocene penguins, the proximal margin of metacarpal I is distinctly separated from the proximal rim of the trochlea carpalis, whereas in Eocene and later penguins it is shifted to nearly the same level. Metacarpal I bears a facet for a free alular digit and extends distally so as to overlap the spatium intermetacarpale, as in *Sequiwaimanu* and later penguins, but unlike in *Muriwaimanu* in which metacarpal I is more proximally restricted. Metacarpal II is straight, lacking the cranial bowing present in Eocene and later penguins. There is no indication of a sulcus tendineus. A wedge-shaped cranial expansion is present at the distal end of metacarpal II. Metacarpal III bears a small, ventrally projecting flange near its proximal end, and projects far distally to metacarpal II, unlike in other Paleocene penguins. As in other Paleocene penguins and the Eocene *Perudyptes*, the articular face of metacarpal II is rounded, whereas it is compressed in more crownward penguins.

A portion of the cranial section of the pelvis is preserved, including part of the synsacrum and the pre-acetabular portion of the right ilium. The ala preacetabularis ilii is quite wide compared to that in modern penguins. The femur lacks the distal condyles, but the preserved section indicates it was slightly longer yet slightly more slender than the femur of the emperor penguin. At the proximal end, the neck is nearly as wide as the head and the fovea ligamentum capitis is oriented dorsomedially as in most penguins (oriented medially in *Crossvallia unienwillia*). The shaft is straight and the crista trochanteris is moderately projected. The proximal portions of the tibiotarsus and fibula are preserved in articulation. The crista cnemialis cranialis has a strong square shape, as in *Crossvallia waiparensis* Mayr et al., 2019, and is more laterally deflected than in extant penguins (Fig. 6.5). The crista cnemialis has a slight proximal hook, which is absent in *Kumimanu*. In both features, the tibiotarsus differs from that of extant penguins and more closely resembles the tibiotarsus of some Procellariiformes.

NMNZ S.47146 (Fig. 6.6, 6.7) closely resembles NMNZ S.46081 in size, the presence of a wide iliac blade, and the proportions of the nearly complete femur. This specimen also preserves two complete thoracic vertebrae and the caudal margin of the scapular blade. The vertebra preserved closest to the synsacrum presumably represents the caudal-most thoracic element. The corpus is weakly opisthocoelous, and a large ovoid fossa is present on the exposed lateral surface (Fig. 6.7). A second weakly opisthocoelous thoracic vertebra is preserved nearby and likely represents the penultimate thoracic element. As in *Kumimanu*, the crista spinosa synsacri is broad and rounded, in contrast to the thinner, sharper shape in modern penguins. The scapular blade is roughly half as wide as the blade in emperor penguins, despite the larger overall size of the specimen, reflecting the lack of the extreme "paddle-like" distal expansion seen in extant penguins.

NMNZ S.47933 (Fig. 6.8–6.10) includes a large number of elements, most of which are incomplete. Three cervical vertebrae and two thoracic vertebrae are preserved. A large portion of the left scapula is preserved, but unfortunately the omal end and caudal end are both missing. The preserved portion of the blade is strap-like. The proximal end of the right humerus is preserved. The intact section is nearly identical in width to the *Petradyptes stonehousei* holotype humerus, and closely resembles it in exhibiting a very wide fossa formed by the impressio m. pectoralis (Fig. 6.9) and a strongly raised insertion scar for m. supracoracoideus that is positioned near the midline of the shaft (Fig. 6.10). The shaft of the humerus is exposed in cross-section slightly distal of the margin of the m. supracoracoideus insertion scar. At a coarse scale, the histological profile resembles that of Eocene penguin humeri from Seymour Island, Antarctica, in having a larger medullary cavity than in modern penguins (Ksepka et al., 2015). The tibiotarsus resembles that of NMNZ S.47146 but is too worn to provide additional information.

NMNZ S.47927 (Fig. 6.11–6.13) includes several elements, most badly truncated. A portion of the femoral shaft is intact and closely matches the size of other specimens provisionally assigned to *Petradyptes stonehousei* (Table 1). Likewise, the width of the distal end of the right carpometacarpus (~20 mm) is consistent with the same measurement in referred specimen NMNZ S.46081 (21.1 mm). As in that specimen, metacarpal II bears a cranial expansion near its distal tip and metacarpal III projects distal to the level of metacarpal II (Fig. 6.13). Metacarpals II and III are both broken so as to expose their cross-section just distal to midshaft, which reveals both are nearly cylindrical as in *Muriwaimanu* and *Sequiwaimanu*, as opposed to the strongly flattened cross-section in more crownward penguins. The medullary cavity is very small in both metacarpals. The scapula is preserved in two sections: the omal portion closely resembles that of *Kumimanu*, and a truncated segment of the blade suggests that it was modestly expanded. The ala postacetabularis ilii is exposed in medial view and tapers to a triangular point. The distal quarter of the left tibiotarsus is preserved in cranial view, although the distal condyles are badly worn. At the level of the break, the shaft is mediolaterally widened as in *Kumimanu biceae* (versus less expanded in crown penguins) and is slightly concave on its cranial face and convex on its caudal face. The medullary cavity is small and surrounded by thick compacta.

Etymology.—In honor of Bernard Stonehouse, in recognition of his landmark contributions to the study of penguins, as well as

https://doi.org/10.1017/jpa.2022.88 Published online by Cambridge University Press

his work on other New Zealand birds and his generous encouragement of fossil penguin researchers.

Material.—NMNZ S.46081: partial sternum, associated ribs, left radiale, complete left carpometacarpus, partial synsacrum and right ilium, right femur missing distal end, and proximal ends of right tibiotarsus and fibula. NMNZ S.47146: two thoracic vertebrae, several ribs, partial scapula, partial pelvis, nearly complete left femur. NMNZ S.47927: fragment of synsacrum, multiple ribs, partial scapula, distal end of right carpometacarpus, postacetabular portion of ilium, femoral shaft, distal end of left tibiotarsus. NMNZ S.47933: three cervical and two thoracic vertebrae, five partial ribs, partial left scapula, proximal end of right humerus, proximal end of right tibiotarsus. One fragment of bone appears to represent part of the sternum but is too incomplete to verify.

Remarks.—Fordyce (1991) briefly described a crushed tibiotarsus (OU 8743), which could potentially belong to *Petradyptes stonehousei*. The width of the distal end of the tibiotarsus is 34.0 mm in OU 8743, which compares well to the width of >30.7 mm (margins partially lost to erosion) in NMNZ S.47927.

Sphenisciformes indet.
Figure 7

Occurrence.—Late Paleocene Moeraki Formation, Hampden Beach, North Otago, New Zealand.

Description.—NMNZ S.46080 includes a fragmentary left humerus, which is missing the distal two thirds of the shaft due to erosion. This exposes the fossa tricipitalis, which is relatively large (Fig. 7.1). A portion of the ventral surface of the head is intact, which reveals that a ridge was present dividing the incisura capitis and sulcus ligamentum transversus (Fig. 7.3). This ridge is present in most Paleocene penguins (e.g., *Muriwaimanu*, *Crossvallia*, *Kupoupou*), although it is absent in *Sequiwaimanu*. Shaft width, which can be measured near the presumed midshaft, is ~90% the length of the species average for king penguins and 105% that of *Sequiwaimanu rosieae*. Accounting for the more slender shaft proportions of Paleocene stem penguins, this suggests an individual intermediate in size between the king penguin and emperor penguin, the two largest extant penguin species. A wide curved element preserved adjacent to the humerus may represent a portion of the furcular ramus.

NMNZ S.47665 (Fig. 7.4) is a right humerus, exposed in longitudinal cross-section. Little information can be gleaned from this specimen other than the fossa tricipitalis appears to have been undivided as in nearly all stem penguins. No meaningful measurements can be obtained, but the overall proportions suggest this humerus was very close in size to NMNZ S.46080.

Material.—NMNZ S.46080: proximal end of left humerus, one rib, and two unidentified fragments of bone. NMNZ S.47665: right humerus lacking distal end.

Remarks.—These specimens are too incomplete to justify erecting a new taxon. We consider it likely they belong to the same species based on size, but this cannot be confirmed due to their incompleteness. Regardless, these smaller fossils support the presence of a fourth distinct penguin species in the Moeraki Formation.

Phylogeny of Paleocene penguins

The parsimony analysis resulted in 7,128 MPTs of 601 steps (CI = 0.628, RI = 0.861, RC = 0.541). The strict consensus tree

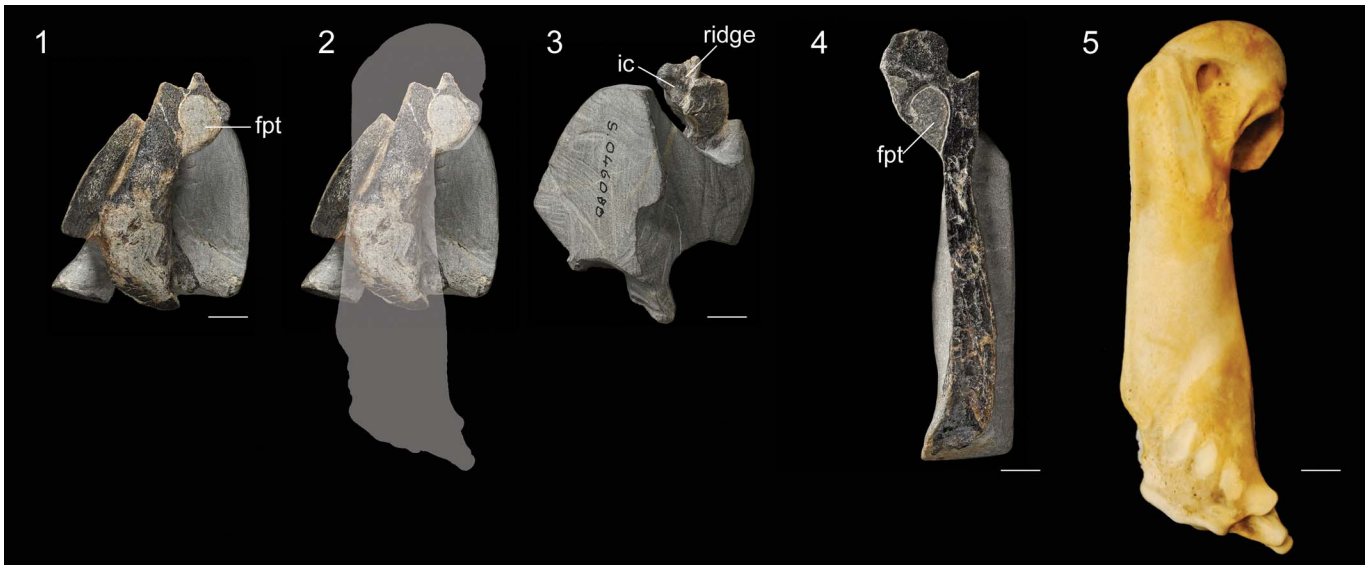

Figure 7. Specimens of Sphenisciformes ident. NMNZ S.46080: (**1**) humerus exposed in partial longitudinal cross-section, (**2**) same image with outline to indicate region preserved and estimated overall size, and (**3**) oblique view of proximal end. NMNZ S.47665: (**4**) humerus exposed in partial longitudinal cross-section. (**5**) Humerus of an extant emperor penguin (*Aptenodytes forsteri*, AMNH 8110) to indicate relative scale. Abbreviations: **ic** = incisura capitis; **fpt** = fossa pneumotricipitalis; **ridge** = ridge dividing the incisura capitis and sulcus ligamentum. Scale bars equal 10 mm.

https://doi.org/10.1017/jpa.2022.88 Published online by Cambridge University Press

(Fig. 8.1) contains a polytomy including *Kumimanu biceae*, *Kumimanu fordycei* n. sp., and a clade uniting *Kaiika maxwelli* and *Petradyptes stonehousei* n. gen. n. sp. The polytomy is recovered one node crownward of a polytomy including *Crossvallia unienwillia* and *Crossvallia waiparensis*, and one node stemward of *Kupoupou stilwelli*. The relationships of the remaining fossil and extant taxa largely conform to previous results (e.g., Degrange et al., 2018; Thomas et al., 2020b), so we focus on the relationships of Paleocene species in the discussion below.

In the parsimony results, a limited number of unambiguous synapomorphies can be identified at each node, due in part to the fact that *Kaiika maxwelli* is known only from the humerus. The clade uniting *Petradyptes*, *Kaiika*, *Kumimanu*, and crownward penguins to the exclusion of *Crossvallia* is united by (174:1) extension of the insertion scar for m. supracoracoideus to the level of the distal rim of the fossa tricipitalis. One additional character state, (240:0) sulcus extensorius of tibiotarsus placed close to midline, represents an ambiguous synapomorphy for this clade because it cannot be scored for *Kaiika* or *Petradyptes*. The clade uniting *Kupoupou* and more crownward penguins to the exclusion of *Petradyptes*, *Kaiika*, and *Kumimanu* is united by three unambiguous characters: (162:0) proximal end of humerus narrow,

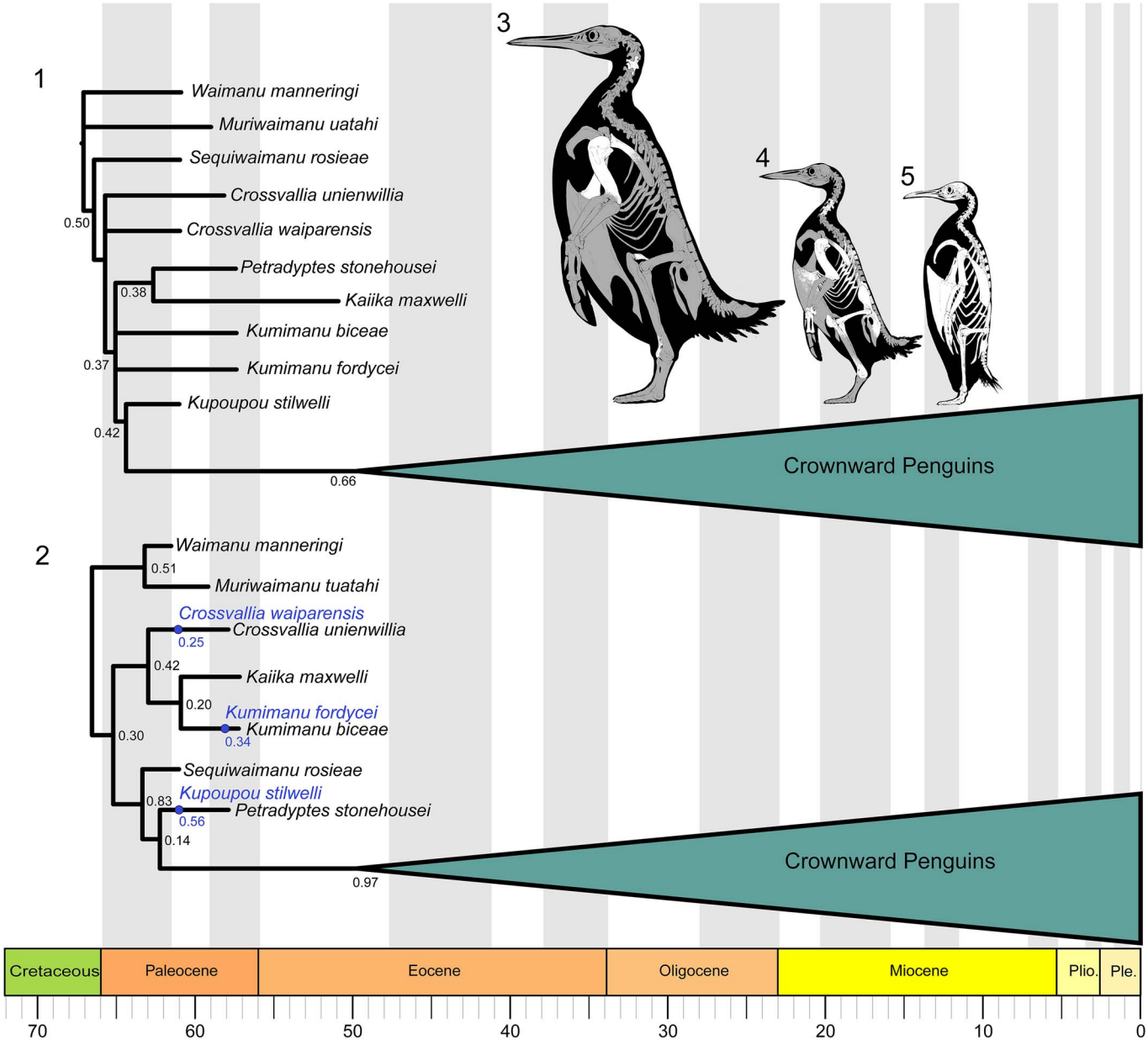

Figure 8. Phylogenetic relationships of Paleocene penguins. (**1**) Strict consensus 7,128 MPTs of 601 steps (CI = 0.628, RI = 0.861, RC = 0.541) from parsimony analysis, with bootstrap support indicated. (**2**) Maximum sampled-ancestor clade credibility tree summarized from the Bayesian combined-evidence analysis in RevBayes. Posterior probabilities are shown for internal nodes. Sampled ancestors are colored blue and posterior probabilities for the MSACC sampled ancestor positions in this tree are shown in blue. Skeletal reconstructions are provided to show the relative sizes of (**3**) *Kumimanu fordycei* n. sp., (**4**) *Petradyptes stonehousei* n. gen. n. sp., and (**5**) the extant emperor penguin *Aptenodytes forsteri*. Bones preserved in the fossil specimens described in this paper are indicated in white. Skeletal reconstructions by Simone Giovanardi.

https://doi.org/10.1017/jpa.2022.88 Published online by Cambridge University Press

(171:1) impressio m. pectoralis forming narrow fossa, and (200:1) processus condylaris dorsalis of ulna reduced. The first two character states, however, constitute reversals. Two features of the tarsometatarsus may represent synapomorphies of *Kupoupou* and more crownward penguins (or a more inclusive clade): (247:2) strongly shortened tarsometatarsus (length <2.5 times width), and (261:1) metatarsal IV straight. The precise distribution of these features cannot be evaluated at present, because the tarsometatarsus remains unknown for *Petradyptes*, *Kaiika*, and *Kumimanu*.

A single character supports the sister group relationship between *Kaiika maxwelli* and *Petradyptes stonehousei*: (160:2) humerus midshaft width more than twice midshaft depth. Although our analysis recovered equally parsimonious topologies uniting *Kumimanu biceae* and *Kumimanu fordycei* in an exclusive clade or placing them as sequential branches along the penguin stem lineage, we consider it much more likely they represent sister taxa based on their very large size and overall similarity. We also note that one character suggests that *Kumimanu* may occupy a slightly more crownward position than *Petradyptes*. As in the stemward taxa *Waimanu*, *Muriwaimanu*, and *Sequiwaimanu*, the caudal thoracic vertebrae of *Petradyptes* bear ovoid lateral depressions. An isolated thoracic vertebra of *Kumimanu biceae* lacks such depressions, as do all more crownward penguins. If this character state were to be confirmed in *Kumimanu fordycei*, it would result in both *Kumimanu* species being shifted to a position one node crownward of *Petradyptes* + *Kaiika*. Likewise, we note that the cnemial crests more closely resemble those of Procellariiformes in *Petradyptes* than in the specimen we tentatively assigned to *Kumimanu biceae*. This feature is not represented by a discrete character in our character matrix, but is also consistent with *Petradyptes* occupying a more basal branch than *Kumimanu*.

Our Bayesian analysis yielded alternate placements for several taxa. In the maximum sampled-ancestor clade credibility (MSACC) tree (Fig. 8.2), the strongest point of conflict with our parsimony analysis regards the placement of *Sequiwaimanu* crownward of *Crossvallia* and *Kumimanu* in the MSACC tree, versus a position near the root of the tree in the parsimony strict consensus tree. Only one character is optimized as supporting the more crownward placement in the MSACC tree: (162:0) humeral proximal width less than twice midshaft depth. *Crossvallia* and *Kumimanu* are both recovered as monophyletic, and *Crossvallia*, *Kumimanu*, and *Kaiika* form a clade as well, unlike in the parsimony result. This clade is supported by one feature, (171:2) impressio m. pectoralis forming a wide fossa (convergently acquired in *Petradyptes*), and is united with all more crownward penguins to the exclusion of *Waimanu* and *Muriwaimanu* by one feature: (256:1) proximal vascular foramina of tarsometatarsus widely separated. *Kupoupou* and *Petradyptes* are potentially supported in a more crownward position than other Paleocene penguins by three features, but all are ambiguous because they cannot be scored in *Sequiwaimanu* or *Petradyptes*: (247:2) tarsometatarsus greatly shortened (length <2.5 times width), (257:0) foramen proximale vascularis medialis opens distal to crista hypotarsi medialis, and (261:1) lateral margin of metatarsal IV straight.

The parsimony tree suffers from several collapsed nodes due to non-overlap of character codings, whereas the MSACC tree is fully resolved, but may present a false sense of precision because many nodes are only weakly supported. Overall, both trees require some homoplasy to explain the distribution of characters related to the flipper morphology of Paleocene penguins. The parsimony tree implies homoplasy in humerus proximal width and the development of the incisura capitis, whereas the Bayesian tree implies homoplasy in the presence of thoracic pleurocoels, shaft flattening, and placement of the insertion for m. supracoracoideus. Both trees also imply homoplasy in the shape of the impressio m. pectoralis. We speculate that discovery of more complete fossils, in particular specimens preserving the distal portions of the flipper and the tarsometatarsus, most likely will result in additional support for placing *Sequiwaimanu* close to the root of the tree as in the parsimony result, but also for the monophyly of the genera *Kumimanu* and *Crossvallia* as in the Bayesian topology.

Body mass in fossil penguins

Regressions.—The humerus of *Kumimanu fordycei* n. sp. is the largest yet reported for a penguin. We developed a set of allometric equations to enable the estimation of penguin body mass from humeral dimensions in order to obtain an estimate of body mass for the new species. An allometric equation in this context is a linear equation fitted to measurements of two independently measured traits after they have been log transformed, sensu Gould (1966) and Riska (1991). Due to a combination of historical inertia and the diagnostic nature of the humerus and tarsometatarsus, the holotypes of almost all fossil penguin species incorporate either one or both of these elements (Marples, 1960; Fordyce and Jones, 1990). Thus, we anticipate that sphenisciform body mass regressions based on humeral dimensions may be of considerable use in future studies.

Previous work exploring forelimb-based body-mass correlates for extant and fossil crown birds did not incorporate penguins or other flightless taxa (Field et al., 2013; Pittman et al., 2020). In order to estimate the original body mass of *Kumimanu fordycei*, three allometric equations were derived using ordinary least squares regression to predict body mass from humerus dimensions in extant penguins, based on measurements obtainable in the *K. fordycei* holotype: maximum humerus proximal width (HPW), maximum humerus length (HL), and humerus midshaft width (HSW).

Our extant penguin body mass dataset includes humerus dimensions from 216 specimens from 20 species, measured using digital calipers sensitive to 0.1 mm. From these specimens we recorded 216 HPW measurements, 214 HL measurements, and 101 HSW measurements. The holotype humerus of *Kumimanu fordycei* measures 233 mm as preserved, however distortion of the head exaggerates its proximal projection (artificial addition estimated at 3.4 mm), and conversely the distal portions of the trochlear ridges are missing (estimated loss of 7 mm length). When these two factors are corrected, we infer a complete length of 236.6 mm.

We gathered body mass data primarily from the species accounts of Borboroglu and Boersma (2013). Penguin body mass is known to fluctuate considerably across the breeding cycle, so it is important to choose a standard point at which to compare values across species. We selected "arrival at colony"

https://doi.org/10.1017/jpa.2022.88 Published online by Cambridge University Press

Table 2. Average body mass and humerus measurements of extant penguins. Body mass is based on average of male and female "arrival at colony" values from Borboroglu and Boersma (2013) unless otherwise indicated. Notes on body mass: 1—Average of "pre-egg laying" Heard Island population. 2—Average of parents of fledging stage chicks. 3—Average of "arrival" females (data on males not available). 4—Species average from Dunning (2008). 5—Average "breeding" weight from Moore et al. (1991) as presented by Williams (1995). 6—Average of "nest building" weight from Williams (1995). 7—Average "breeding" weight from Williams (1995). 8—Weights listed as "wild penguins at colony" potentially including post-arrival individuals. 9—Average body mass at arrival from 5-year survey reported in Williams (1995). 10—Mid-incubation values from Williams (1995). Body mass reported in kilograms. Humerus measurements reported in millimeters, taken directly. Regression analyses used the natural log of species-averaged body mass against the natural log of humerus measurements from individual birds and not the species-averaged humerus measurements shown here.

Taxon	Mean mass	N	Maximum humerus length (HL)	Maximum humerus head width (HHW)	Humerus midshaft width (HMW)
Aptenodytes forsteri	32.55	16	133.9	41.0	26.2
Aptenodytes patagonicus	13.24	9	113.9	33.5	22
Eudyptes chrysocome	2.98	2	68.2	20.2	10.7
Eudyptes chrysolophus[1]	5.02	11	74.8	22.3	15.4
Eudyptes filholi	2.98	7	60.5	17.8	—
Eudyptes moseleyi	3.04	1	60.7	17.5	12.1
Eudyptes pachyrhynchus	4.1	21	66.3	19.1	14.1
Eudyptes robustus[2]	3.002	19	65.0	18.6	13.6
Eudyptes schlegeli	5.2	4	75.2	22.6	18.9
Eudyptes sclateri[3]	5.56	16	73.3	21.9	—
Eudyptula minor[4]	1.12	35	45.9	12.1	7.9
Eudyptula novaehollandiae[4]	1.11	5	48.1	12.7	8.2
Megadyptes antipodes[5]	5.1	14	77.4	22.8	16.6
Pygoscelis adeliae	4.98	10	73.6	22.0	15.4
Pygoscelis antarctica	4.73	6	71.5	21.0	15.8
Pygoscelis papua[6]	5.36	8	86.4	24.6	18.6
Spheniscus demersus[7]	3.05	14	68.8	19.4	12.2
Spheniscus humboldti[8]	4.38	7	73.5	21.9	15.0
Spheniscus magellanicus[9]	4.82	8	73.5	20.8	14.2
Spheniscus mendiculus[10]	1.93	3	58.0	17.0	11.4

masses for this purpose both because it represents a relatively discrete time interval in the breeding cycle, and because body masses for penguins are often obtained at this stage because researchers can capture penguins easily when they are on land. Sources for species for which body masses at the arrival at colony stage were not available from Borboroglu and Boersma (2013) are listed in Table 2. The natural log of species-averaged body mass was used against the natural log of humerus measurements from individual birds in the regression analyses.

The largest previously reported penguin humerus belongs to the holotype specimen of *Kumimanu biceae*. This specimen lacks an indeterminate portion of its distal end, which resulted in estimates of its total length ranging from 185 mm to 228 mm based on extrapolations using the humerus proportions of other stem penguins (Mayr et al., 2017a). If the proportions of *Kumimanu biceae* matched those of *Kumimanu fordycei*, the humerus of the former would have approached the upper range of these estimates at 218 mm maximum length. We used this length when estimating the body mass of *K. biceae*. Mass estimates for these and other "giant" penguins analyzed in this study represent extrapolations from our regression models, due to the exceptionally large sizes of these fossils relative to extant penguins.

Mass estimates.—The strength of correlation between skeletal measurements and body mass was assessed with a coefficient of determination (R^2) obtained from ordinary least squares regression. Maximum humerus proximal width and maximum humerus length provided accurate estimates of body mass in extant penguins (both exhibiting R^2 of 0.95). Both relationships were significant, with p-values <0.001. All emperor penguin specimens had high leverage on the HPW regression based on hat matrix values, and all emperor and several king penguin and *Eudyptula* specimens had high leverage on the HL regression. The equation we derived for estimating body mass (BM) from measurements of maximum humerus proximal width is:

$$\mathrm{Ln(BM)} = 2.5857(\mathrm{Ln(HPW)}) + 0.5394$$

The equation derived for maximum humerus length is:

$$\mathrm{Ln(BM)} = 2.9613(\mathrm{Ln(HL)}) - 4.2823$$

Mean body mass estimates derived for *Kumimanu fordycei* were 159.7 kg based on maximum humerus proximal width (142.6 kg and 178.8 kg as the lower and upper 95% confidence interval bounds, respectively), and 148.0 kg based on maximum humerus length (132.5 kg and 165.3 kg, lower and upper 95% confidence interval bounds, respectively). We therefore estimate that this species would have exhibited a colony arrival mass in the range of ~155 kg when alive—thus ranking as the heaviest penguin yet discovered.

We also calculated a body mass regression based on humerus midshaft width:

$$\mathrm{Ln(BM)} = 2.5849(\mathrm{Ln(HSW)}) + 1.5219$$

Our regression based on midshaft width yielded a poorer fit (R^2 = 0.8843, p-value <0.001) than those based on humerus length or proximal width, and resulted in a much lower body mass estimate of 66.3 kg for *Kumimanu fordycei*. Beyond the reduced fit of this equation, as indicated by its lower R^2 value, this midshaft width regression will inevitably be biased towards erroneously low estimates of body size for early stem penguins, in which the humeral shaft is less flattened than in later penguins including the crown

https://doi.org/10.1017/jpa.2022.88 Published online by Cambridge University Press

Table 3. Comparative dimensions of fossil penguin humeri. Sources for specimens not measured directly: 1—Jadwiszczak, 2006; 2—Mayr et al., 2017a; 3—Acosta Hospitaleche et al., 2017; 4—Acosta Hospitaleche, 2005; 5—Jadwiszczak et al., 2013; 6—Mayr et al., 2019; 7—Simpson, 1981; 8—Chávez Hoffmeister et al., 2014; 9—Acosta Hospitaleche, 2014; 10—Chávez Hoffmeister, personal communication, 2016; 11—Emslie et al.,2003; 12—Göhlich, 2007. *The humerus is weathered and has lost at least part of the periosteum, so this value may be a modest underestimate of true width and hence body mass. **Note the table of Mayr et al., 2017a, indicates a width of 70 mm whereas the text (Mayr et al., 2017a, p. 4) indicates 75 mm. The latter value is correct.

Taxon	Specimen	Length (mass estimate)	Head width (mass estimate)	Midshaft width (mass estimate)
Anthropodyptes gilli	AMNH 7609 (cast)	~165.0 mm (50.9 kg)	—	30.4 mm (31.2 kg)
Anthropornis nordenskjoeldi	IB/P/B−0119[1]	152.2 mm (40.1 kg)	—	—
Anthropornis nordenskjoeldi	MLP 83-1-1-190[2]	181.0 mm (67 kg)	57.0 mm (59.5 kg)	—
Aprosdokitos mikrotero	MLP-00-I-I-19[3]	—	—	6.8 mm* (0.7 kg)
Archaeospheniscus lowei	OM GL407	128.0 mm (24.0 kg)	—	—
Arthrodytes andrewsi	MLP 606[4]	142.0 mm (32.6 kg)	—	—
Burnside "*Palaeeudyptes*"	OM GL435	157.0 mm (43.9 kg)	—	30.0 mm (30.1 kg)
Crossvallia unienwillia[5]	MLP 00-I-10-1	170.9 mm (56.5 kg)	~53.0 mm (49.3 kg)	23.8 mm (16.6 kg)
cf. *Crossvallia waiparensis*[6]	CM 2016.158.3	—	48.5 mm (39.2 kg)	—
Eretiscus tonnii[7]	MLP 81-VI-26-1	40.8 mm (0.8 kg)	—	—
Eudyptes atatu	NMNZ S.46320	71.9 mm (4.3 kg)	22.6 mm (5.4 kg)	15.6 mm (5.6 kg)
Eudyptes calaunia[8]	SGO-PV 21451	—	—	17.4 mm (7.4 kg)
Eudyptes warhami	NMNS S.25157	69.1 mm (3.9 kg)	—	—
Icadyptes salasi	MUSM 897	167 mm (52.8 kg)	61.7 mm (73.0 kg)	36.1 mm (48.16 kg)
Inguza predemersus	SAM PQ-L 6510	56.5 mm (2.1 kg)	—	9.2 mm (1.4 kg)
Inkayacu paracasensis	MUSM 1444	161.6 mm (47.9 kg)	—	29.1 mm (27.9 kg)
Kaiika maxwelli	OU 22402	146.8 mm* (36.0 kg)	42.1 mm (27.2 kg)	22.0 mm (13.5 kg)
Kairuku grebneffi	OU 22065	176.6 mm (62.3 kg)	55.5 mm (55.5 kg)	30.5 mm (31.5 kg)
Kairuku waewaeroa	WM 2006/1/1	185 mm (71.4 kg)	53.5 mm (50.5 kg)	31.0 mm (32.8 kg)
Kumimanu biceae	NMNZ S.45877	~218 mm (116.1 kg)	75.0 mm** (121.0 kg)	~33.0 mm (38.6 kg)
Kumimanu fordycei n. sp.	NMNZ S.47426	~236.6 mm (148.0 kg)	~83.5 mm (159.7 kg)	40.7 mm (66.3 kg)
Kupoupou stilwelli	NMNZ S.47308	106.8 mm (14.0 kg)	18.6 mm (3.3 kg)	14.4 mm (4.5 kg)
Madrynornis mirandus	MEF−PV 100	79.1 mm (5.8 kg)	21.5 mm (4.8 kg)	13.6 mm (3.9 kg)
Marplesornis novaezealandiae	CM Zfa-4	101.5 mm (12.1 kg)	—	20.5 mm (11.3 kg)
Muriwaimanu tuatahi	CM zfa 34	109.6 mm (15.2 kg)	—	11.0 mm (2.3 kg)
Pachydyptes ponderosus	NMNZ OR.1450	179.6 mm (65.4 kg)	68.2 mm (94.6 kg)	44.1 mm (81.6 kg)
Palaeeudyptes klekowskii	UCMP 321023	~164 mm (50.0 kg)	—	26.5 mm (21.9 kg)
cf. *Palaeeudyptes klekowskii*[9]	MLP 12-I-20-288	—	65.2mm (84.2kg)	—
Palaeospheniscus bergi[10]	MLP 97-VI-1-2	67.0 mm (3.5 kg)	—	—
Palaeospheniscus biloculata[10]	MLP 20-565	90.3 mm (8.5 kg)	—	—
Palaeospheniscus patagonicus[10]	MLP 20-68	77.6 mm (5.5 kg)	—	—
Paraptenodytes antarcticus	AMNH 3338	114.1 mm (17.1 kg)	—	17.7 mm (7.7 kg)
Perudyptes devriesi	MUSM 889	~120 mm (19.8 kg)	31.5mm (12.8 kg)	18.5 mm (8.6 kg)
Petradyptes stonehousei n. gen. n. sp.	NMNZ S.47114	—	53.4 mm (50.3 kg)	30.4 mm (31.2 kg)
Platydyptes amiesi	OM GL434	118.1 mm (18.9 kg)	41.2 mm (25.7 kg)	28.5 mm (26.4 kg)

https://doi.org/10.1017/jpa.2022.88 Published online by Cambridge University Press

Table 3. Continued.

Taxon	Specimen	Length (mass estimate)	Head width (mass estimate)	Midshaft width (mass estimate)
Platydyptes marplesi	OM GL2317	88.8 mm (8.1 kg)	—	~22.0 mm (13.5 kg)
Platydyptes novaezealandiae	NMNZ OR.1451	103.1 mm (12.6 kg)	33.0 mm (14.5 kg)	23.0 mm (15.2 kg)
Pygoscelis tyreei	CM zfa22631	89.2 mm (8.2 kg)	—	—
Sequiwaimanu rosieae	CM 2016.6.1	126.2 mm (23.0 kg)	33.7 mm (15.3 kg)	19.0 mm (9.3 kg)
Spheniscus chilensis[11]	UCN-1-130697	72.2 mm (4.4 kg)	20.3 mm (4.1 kg)	13.0 mm (3.5 kg)
Spheniscus muizoni[12]	MNHN PPI 147	74.0 mm (4.7 kg)	22.8 mm (5.6 kg)	—
Spheniscus urbinai	MUSM 402	106.5 mm (13.9 kg)	32.4 mm (13.8 kg)	—

group, resulting in a greater thickness but a lesser width for a given overall size. This results in a large disparity between estimates from midshaft width and other indices for early stem penguins (e.g., the mass estimates from humerus length and humerus proximal width are more than six times greater than the estimate from midshaft width for *Muriwaimanu*). We therefore consider results from the midshaft width regression unreliable for estimating the body masses of Paleocene stem penguins such as those described here. Body mass estimates from all three regressions for 40 fossil taxa are presented in Table 3.

Discussion

Intriguingly, some of the features of the humerus that distinguish *Kumimanu* and *Petradyptes* n. gen. from more crownward penguins resemble those in volant underwater divers such as diving petrels (Procellariiformes: *Pelecanoides*) and auks (Charadriiformes: Alcidae) (e.g., Smith, 2011; Mayr et al., 2020; Watanabe et al., 2021). Similarities between the flight musculature of Paleocene penguins, diving petrels, and alcids are suggested by development of the insertion scars of key muscles involved in the upstroke and downstroke, including the wide impressio m. pectoralis, strongly raised insertion scar for m. supracoracoideus, and less distally elongated insertion scar for m. supracoracoideus scar (Figs. 9, 10). Although not well described, the m. latissimus dorsi scar in early Paleocene penguins appears to have resembled that of auks in being weak and lineate, as opposed to the strong circular insertion observed in later penguins (best observed in *Sequiwaimanu*). These similarities to distantly related taxa capable of both aerial flight and wing-propelled diving suggest that despite being clearly flightless, early giant penguins such as *Kumimanu* may have retained some ancestral features that were once necessary for aerial flight but less optimal for underwater flight. Thus, it is likely that Paleocene stem penguins employed an underwater flight stroke that was less efficient than that of later penguins. Testing this idea quantitatively will require future functional analyses.

Previous attempts to estimate body mass for extinct penguins relied primarily on hindlimb elements (Jadwiszczak, 2001; Jadwiszczak and Mörs, 2011). While hindlimb

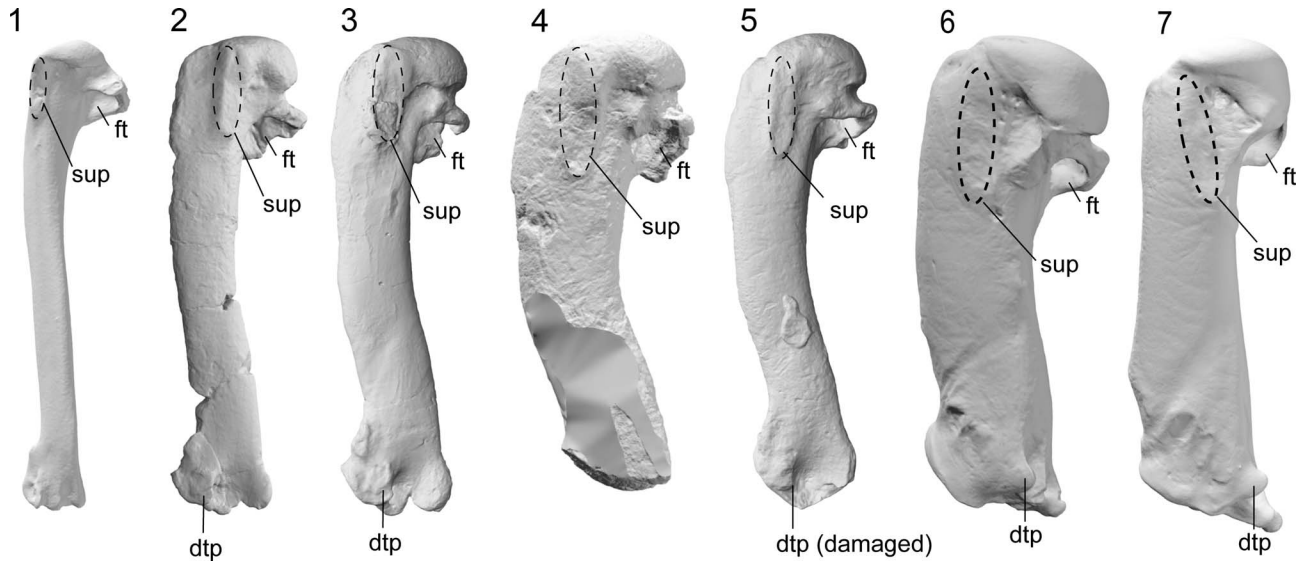

Figure 9. Comparative images of the humerus in dorsal view (swimming posture): (**1**) the auk (Alcidae) *Alca torda* Linnaeus, 1758 (NMNZ OR.12282) and the penguins (**2**) *Muriwaimanu tuatahi* (OU12651), (**3**) *Sequiwaimanu rosieae* (CM 2016.6.1), (**4**) *Petradyptes stonehousei* n. gen. n. sp. (NMNZ S. 47114), (**5**) *Kaiika maxwelli* (OU22402), (**6**) *Pachydyptes ponderosus* (NMNZ OR.1450), and (**7**) *Aptenodytes forsteri* (NMNZ OR.23039). Abbreviations: **dtp**, dorsal trochlear process; **ft,** fossa tricipitalis; **sup**, insertion scar for m. supracoracoideus. Not to scale.

https://doi.org/10.1017/jpa.2022.88 Published online by Cambridge University Press

dimensions are indeed useful for estimating avian body masses (e.g., Campbell and Marcus, 1992; Field et al., 2013), many of the largest reported penguin specimens do not preserve hindlimb material. Our regressions suggest that humerus dimensions also provide reliable estimates of body mass for penguins. Because the underwater flight stroke provides the primary means of penguin locomotion, there is good reason to suspect that the humerus, which serves as the primary attachment point for the major muscles involved in the upstroke and downstroke, may scale relatively tightly to the body mass of the bird that the muscles must propel through the water.

The humerus of *Kumimanu fordycei* n. sp. is the largest penguin humerus yet discovered, both in terms of its overall length and proximal width. Only the late Eocene *Pachydyptes ponderosus* Oliver, 1930, has a larger midshaft width, but this primarily reflects the proportionally wider shaft of post-Paleocene taxa (Table 3).

Other very large penguins also have been reported from different elements. The largest previously reported penguin hindlimb element is an isolated tarsometatarsus (MLP 12-I-20-288) from the Eocene La Meseta Formation of Seymour Island, Antarctica. This specimen was assigned to *Palaeeudyptes klekowskii* Myrcha, Tatur, and del Valle 1990, by Acosta Hospitaleche (2014), and is ~25% longer than the holotype tarsometatarsus of *P. klekowskii*, which itself is one of the largest specimens previously known for the species. If correctly referred, this would imply a surprisingly wide range of intraspecific size variation. Regardless of its taxonomic affinities, MLP 12-I-20-288 clearly belonged to an extremely large penguin. Applying regressions based on tarsometatarsus width and depth (Jadwiszczak, 2001), Acosta Hospitaleche (2014) estimated a body mass of 114.4–116.2 kg for this individual. A large partial humerus, preserving only its proximal end (MLP- 12-I-20-288), was also assigned to *Palaeeudyptes klekowskii* in the same study. Because these bones cannot be directly associated, it remains possible that they belong to two different species, or at least to individuals of different sizes. Our regression based on humerus proximal width (65.2 mm in MLP- 12-I-20-288) yields a body mass estimate of 84.2 kg. In terms of overall length of the humerus itself, scaling using the proportions of smaller complete *Palaeeudyptes klekowskii* humeri suggests a total length of ~226 mm for this specimen, which would be ~90% the length of the *Kumimanu fordycei* holotype humerus.

In summary, available comparisons support *Kumimanu fordycei* as the heaviest known penguin. Future discovery of tarsometatarsi belonging to *Kumimanu* would allow us to compare mass estimates from Jadwiszczak's (2001) regression directly with those from the large *Palaeeudyptes* tarsometatarsus. We refrain from attempting comparisons of standing height or body length among these taxa, given that very different proportions of stem and crown penguins make such inferences difficult in the absence of nearly complete skeletons (Ksepka et al., 2012).

Nevertheless, the giant body sizes of many stem penguins suggest a foraging niche that is not found in any aquatic bird group today. Because some Paleocene penguins attained giant body size while retaining plesiomorphic flipper features, we speculate that the rapid shift to giant sizes in Paleocene penguins may have been driven primarily by selection for more efficient thermoregulation. Larger endotherms are able to maintain body temperature more efficiently through thermal inertia, and there is a clear positive correlation between body size and both dive depth and dive duration in marine birds (e.g., Boyd and Croxall, 1996; Watanuki and Burger, 1999; Halsey et al., 2006). Giant size may have allowed *Kumimanu* penguins to gain access to foraging areas in colder and deeper waters and to exploit larger prey than smaller contemporaneous penguin taxa.

Although their overall range of body sizes is much lower, the fact that penguins reached their overall peak in body size very early in their evolutionary history stands in marked contrast to patterns observed among marine mammals. Fossil pinnipeds

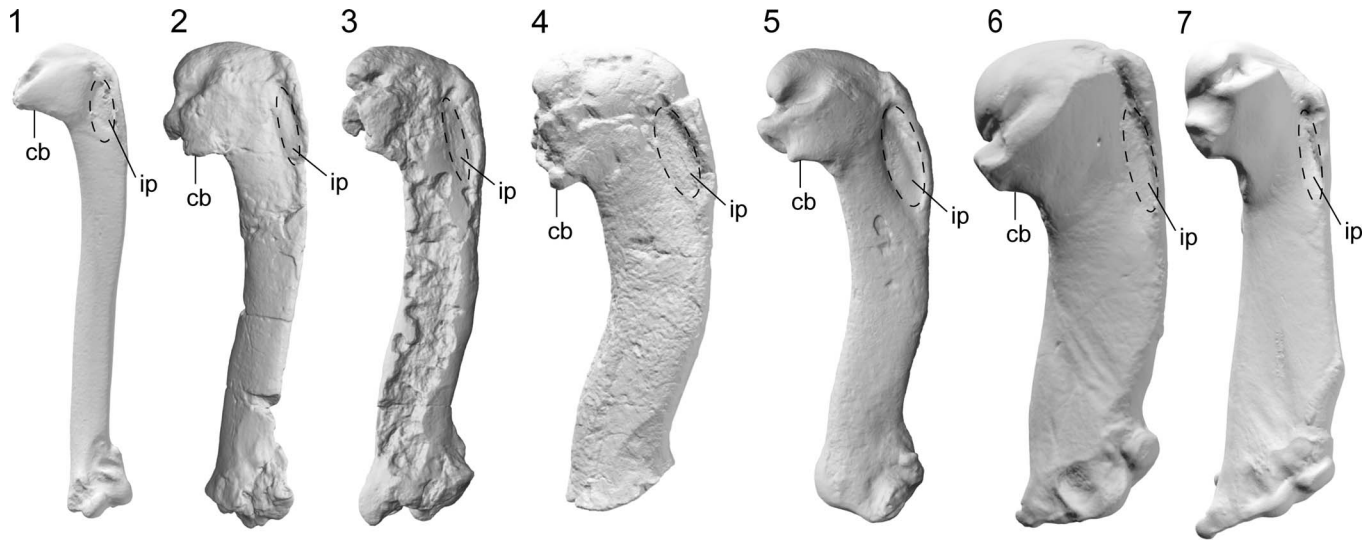

Figure 10. Comparative images of the humerus ventral view (swimming posture): (**1**) the auk (Alcidae) *Alca torda* (NMNZ OR.12282) and the penguins (**2**) *Muriwaimanu tuatahi* (OU12651), (**3**) *Sequiwaimanu rosieae* (CM 2016.6.1), (**4**) *Petradyptes stonehousei* n. gen. n. sp. (NMNZ S. 47114), (**5**) *Kaiika maxwelli* (OU22402), (**6**) *Pachydyptes ponderosus* (NMNZ OR.1450), and (**7**) *Aptenodytes forsteri* (NMNZ OR.23039). Abbreviations: **cb**, crista bicipitalis, **ip**, impressio m. pectoralis. Not to scale.

https://doi.org/10.1017/jpa.2022.88 Published online by Cambridge University Press

date to the Oligocene but the clade did not reach their peak body sizes until the late Miocene, sirenians date to the early Eocene but did not reach peak body sizes until the Pliocene, and cetaceans date to the early Eocene but only reached peak body size close to the present (Churchill et al., 2015; Pyenson and Vermeij, 2016). The unusual trajectory of body size evolution in penguins may be explained in part by the fact that penguins never approached the upper size limits of their marine mammal counterparts, limited by factors such as ovipary. However, another possible factor is that penguins were likely already highly adapted to marine diving before they lost flight, given that all evidence suggests the earliest stem penguins would have been volant wing-propelled divers similar to auks (Simpson, 1946). Thus, the loss of flight would have opened the door for rapid body size increases by removing the competing pressure for limiting weight for take-off.

The early attainment of giant body size by penguins also may have allowed them to take advantage of a limited window of opportunity, which closed as pinnipedimorphs spread through the southern oceans. Giant penguins vanished near the Oligocene-Miocene boundary, and one favored hypothesis is that predation pressure or competition from pinnipedimorphs for food and breeding sites led to selective extinction of very large species whereas smaller penguins thrived from the Miocene onwards (Warheit and Lindberg, 1988; Warheit, 1992). The lack of spatiotemporal overlap between the largest known fossil penguins and similar-sized marine mammals is consistent with this hypothesis (Ando and Fordyce, 2014).

An underappreciated aspect of the early evolution of giant body size in penguins is the potential for improved thermoregulation to increase long-distance dispersal capabilities. Earlier work suggested that penguins originated in Zealandia and dispersed to other continents only after the evolution of the humeral plexus (Thomas et al., 2011). This plexus is only one of several countercurrent heat exchangers present in extant penguins, but is emphasized in paleobiological studies because it is the only one that leaves an osteological correlate that can serve as a proxy of presence/absence in fossil taxa (Thomas et al., 2011). With increasing evidence that giant size also originated while penguins were still restricted to Zealandia, it is interesting to note that the earliest record of a penguin on another continent is the giant *Crossvallia unienwillia* from Antarctica (Tambussi et al., 2005). The humerus of this species is too poorly preserved to infer whether the humeral plexus was present, but the absence of evidence for this structure in *Petradyptes*, *Kaiika*, and *Kupoupou* suggests that the humeral plexus evolved after *Crossvallia* had already diverged from other penguins. Thus, it is possible that the thermoregulatory benefits of large body size facilitated some key dispersal events in Paleocene penguins, allowing these early titans to explore a wider range of both geographical and ecological space.

Acknowledgments

We thank R.E. Fordyce (OU), R.P. Scofield (CM), M. Florence and H. James (USNM), C. Mehling, M. Norell, J. Cracraft, P. Capainolo, B. Smith, and P. Sweet (AMNH), and R. Prum and K. Zyskowski (YPM) for access to specimens; S. Tennyson, A. Mannering, and J. Wold for their help in finding the Hampden Beach fossils described here; and A. Mannering also for his outstanding work preparing the new specimens. We thank P. Jadwiszczak for sharing photos of Antarctic fossil specimens, K. Dzikiewicz for collecting measurements, C. Kammerer for advice on Greek etymology, and J.-C. Stahl for photography of the new Hampden Beach fossils. DTK was supported by National Science Foundation award DEB-1556615. DJF is supported by UKRI Future Leaders Fellowship MR/S032177/1. TAH and WP were supported by NSF DBI-1759909. The Te Papa Collection Development Fund supported fieldwork, fossil preparation, and storage.

Data availability statement

The morphological dataset and all scripts used for phylogenetic analyses in this study are available from the Dryad Digital Repository: https://doi.org/10.5061/dryad.ttdz08m1r.

References

Acosta Hospitaleche, C., 2005, Systematic revision of *Arthrodytes* Ameghino, 1905 (Aves, Spheniscidae) and its assignment to the Paraptenodytinae: Neues Jahrbuch für Geologie und Paläontologie, Abhandlungen, v. 7, p. 404–414.

Acosta Hospitaleche, C., 2014, New giant penguin bones from Antarctica: systematic and paleobiological significance: Comptes Rendus Palevol, v. 13, p. 555–560.

Acosta Hospitaleche, C., Reguero, M., and Santillana, S., 2017, *Aprosdokitos mikrotero* gen. et sp. nov., the tiniest Sphenisciformes that lived in Antarctica during the Paleogene: Neues Jahrbuch für Geologie und Paläontologie, Abhandlungen, v. 283, p. 25–34.

Ando, T., and Fordyce, R.E., 2014, Evolutionary drivers for flightless, wing-propelled divers in the Northern and Southern hemispheres: Palaeogeography, Palaeoclimatology, Palaeoecology, v. 400, p. 50–61.

Baumel, J.J., and Witmer, L.M., 1993, Osteologia, *in* Baumel, J.J., King, A.S., Breazile, J.E., Evans, H.E., and Vanden Berge, J.C., eds., Handbook of Avian Anatomy: Nomina Anatomica Avium: Cambridge, Massachusetts, Nuttall Ornithology Club, p. 45–132.

Bertelli, S., and Giannini, N.P., 2005, A phylogeny of extant penguins (Aves: Sphenisciformes) combining morphology and mitochondrial sequences: Cladistics, v. 21, p. 209–239.

Blender Online Community, 2022, Blender—a 3D modelling and rendering package. Blender Foundation, Stichting Blender Foundation, Amsterdam. http://www.blender.org.

Blokland, J.C., Reid, C.M., Worthy, T.H., Tennyson, A.J.D., Clarke, J.A., and Scofield, R.P., 2019, Chatham Island Paleocene fossils provide insight into the palaeobiology, evolution, and diversity of early penguins (Aves, Sphenisciformes): Palaeontologia Electronica, v. 22, 22.3.78. https://doi.org/10.26879/1009.

Boyd, I.L., and Croxall, J.P., 1996, Dive durations in pinnipeds and seabirds: Canadian Journal of Zoology, v. 74, p. 1696–1705.

Borboroglu, P.G., and Boersma, P.D., 2013, Penguins: Natural History and Conservation: Seattle, University of Washington Press, 360 p.

Campbell, K.E., Jr., and Marcus, L., 1992, The relationship of hindlimb bone dimensions to body weight in birds: Natural History Museum of Los Angeles County, Science Series, v. 36, p. 395–412.

Chávez Hoffmeister, M., Carrillo Briceño, J.D, and Nielsen, S.N., 2014, The evolution of seabirds in the Humboldt Current: new clues from the Pliocene of Central Chile: PLoS ONE, v. 9, e90043. https://doi.org/10.1371/journal.pone.0090043.

Churchill, M., Clementz, M.T., and Kohno, N., 2015, Cope's rule and the evolution of body size in Pinnipedimorpha (Mammalia: Carnivora): Evolution, v. 69, p. 201–215.

Clarke, J.A., Ksepka, D.T., Stucchi, M., Urbina, M., Giannini, N., Bertelli, S., Narváez, Y., and Boyd, C.A., 2007, Paleogene equatorial penguins challenge the proposed relationship between biogeography, diversity, and Cenozoic climate change: Proceedings of the National Academy of Sciences, v. 104, p. 11545–11550.

Cole, T.L., Ksepka, D.T., Mitchell, K.J., Tennyson, A.J.D., Thomas, D.B., et al., 2019, Mitogenomes uncover extinct penguin taxa and reveal island formation as a key driver of speciation: Molecular Biology and Evolution, v. 36, p. 784–797.

https://doi.org/10.1017/jpa.2022.88 Published online by Cambridge University Press

Crouch, E.M., and Brinkhuis, H., 2005, Environmental change across the Paleocene–Eocene transition from eastern New Zealand: a marine palynological approach: Marine Micropaleontology, v. 56, p. 138–160.
Degrange, F.D., Ksepka, D.T., and Tambussi, C.P., 2018, Redescription of the oldest crown clade penguin: cranial osteology, jaw myology, neuroanatomy, and phylogenetic affinities of *Madrynornis mirandus*: Journal of Vertebrate Paleontology, v. 38, e1445636. https://doi.org/10.1080/02724634.2018.1445636.
Dunning, J.B., Jr., 2008, CRC Handbook of Avian Body Masses, 2nd Edition: Boca Raton, CRC Press, 666 p.
Emslie, S.D., and Guerra Correa, C., 2003, A new species of penguin (Spheniscidae: *Spheniscus*) and other birds from the Late Pliocene of Chile: Proceedings of the Biological Society of Washington, v. 50, p. 1–113.
Field, D.J., Lynner, C., Brown, C., and Darroch, S.A.F., 2013, Skeletal correlates for body mass estimation in modern and fossil flying birds: PLoS ONE, v. 8, e82000. https://doi.org/10.1371/journal.pone.0082000.
Fordyce, R.E., 1991, A new look at the fossil vertebrate record of New Zealand, *in* Vickers-Rich, P., Monaghan, J.M., Baird, R.F., and Rich, T.H., eds., Vertebrate Palaeontology of Australasia: Melbourne, Pioneer Design Studio and Monash University, p. 1191–1316.
Fordyce, R.E., and Jones, C.M., 1990, Penguin history and new fossil material from New Zealand, *in* Davis, L.S., and Darby, J.T., eds., Penguin Biology: San Diego, Academic Press, p. 419–446.
Fordyce, R.E., and Thomas, D.B., 2011, *Kaiika maxwelli*, a new Early Eocene archaic penguin (Sphenisciformes, Aves) from Waihao Valley, South Canterbury, New Zealand: New Zealand Journal of Geology and Geophysics, v. 54, p. 43–51.
Giovanardi, S., Ksepka., D.T., and Thomas, D.B., 2021, A giant Oligocene fossil penguin from the North Island of New Zealand: Journal of Vertebrate Paleontology, v. 41, e1953047. https://doi.org/10.1080/02724634.2021.1953047.
Göhlich, U.B., 2007, The oldest fossil record of the extant penguin genus *Spheniscus*—a new species from the Miocene of Peru: Acta Paleontologica Polonica, v. 52, p. 285–298.
Gould, S.J., 1966, Allometry and size in ontogeny and phylogeny: Biological Reviews of the Cambridge Philosophical Society, v. 41, p. 587–640.
Gray, G.R., 1844, *Aptenodytes*: The Annals and Magazine of Natural History, v. 13, p. 315.
Halsey, L.G., Blackburn, T.M., and Butler, P., 2006, A comparative analysis of the diving behaviour of birds and mammals: Functional Ecology, v. 20, p. 889–899.
Huxley, T.H., 1859, On a fossil bird and a fossil cetacean from New Zealand: Quarterly Journal of the Geological Society, v. 15, p. 670–677.
Heath, T.A., Huelsenbeck, J. P., and Stadler, T., 2014, The fossilized birth-death process for coherent calibration of divergence-time estimates: Proceedings of the National Academy of Sciences, v. 111, p. E2957–E2966.
Höhna, S., Landis, M.J., Heath, T.A., Boussau, B., Lartillot, N., Moore, B.R., Huelsenbeck, J.P., and Ronquist, F., 2016, RevBayes: Bayesian phylogenetic inference using graphical models and an interactive model-specification language: Systematic Biology, v. 65, p. 726–736.
Jadwiszczak, P., 2001, Body size of Eocene Antarctic penguins: Polish Polar Research, v. 22, p. 147–158.
Jadwiszczak, P. 2006. Eocene penguins of Seymour Island, Antarctica: taxonomy: Polish Polar Research, v. 27, p. 3–62.
Jadwiszczak, P., and Mörs, T., 2011, Aspects of diversity in early Antarctic penguins: Acta Palaeontologica Polonica, v. 56, p. 269–277.
Jadwiszczak, P., Acosta Hospitaleche, C., and Reguero, M., 2013, Redescription of *Crossvallia unienwillia*: the only Paleocene Antarctic penguin: Ameghiniana, v. 50, p. 545–553.
Ksepka, D.T., Bertelli, S., and Giannini, N.P., 2006, The phylogeny of the living and fossil Sphenisciformes (penguins): Cladistics, v. 22, p. 412–441.
Ksepka, D.T., Clarke, J.A., DeVries, T.J., and Urbina, M., 2008, Osteology of *Icadyptes salasi*, a giant penguin from the Eocene of Peru: Journal of Anatomy, v. 213, p. 131–147.
Ksepka, D.T., Fordyce, R.E., Ando, T., and Jones, C.M., 2012, New fossil penguins (Aves: Sphenisciformes) from the Oligocene of New Zealand reveal the skeletal plan of stem penguins: Journal of Vertebrate Paleontology, v. 32, p. 235–254.
Ksepka, D.T., Werning, S., Sclafani, M., and Boles, Z.M., 2015, Bone histology in extant and fossil penguins (Aves: Sphenisciformes): Journal of Anatomy, v. 227, p. 611–630.
Lartillot, N., and Philippe, H., 2004, A Bayesian mixture model for across-site heterogeneities in the amino-acid replacement process: Molecular Biology and Evolution, v. 21, p. 1095–1109.
Linnaeus, C., 1758, Systema Naturæ per regna tria naturæ, secundum classes, ordines, genera, species, cum characteribus, differentiis, synonymis, locis. Tomus I. Editio decima, reformata: Holmiæ, Salvius, 824 p.
Marples, B.J., 1952, Early Tertiary penguins of New Zealand: New Zealand Geological Survey Paleontological Bulletin, v. 20, p. 1–66.
Marples, B.J., 1960, A fossil penguin from the Late Tertiary of North Canterbury: Records of the Canterbury Museum, v. 7, p. 185–195.
Mayr, G., Scofield, R.P., De Pietri, V.L., and Tennyson, A.J.D., 2017a, A Paleocene penguin from New Zealand substantiates multiple origins of gigantism in fossil Sphenisciformes: Nature Communications, v. 8, 1927. https://doi.org/10.1038/s41467-017-01959-6.
Mayr, G., De Pietri, V.L., Love, L., Mannering, A.A., and Scofield, R.P., 2017b, A well-preserved new mid-Paleocene penguin (Aves, Sphenisciformes) from the Waipara Greensand in New Zealand: Journal of Vertebrate Paleontology, v. 37, e1398169. https://doi.org/10.1080/02724634.2017.1398169.
Mayr, G., De Pietri, V.L., Love, L., Mannering, A.A., and Scofield, R.P., 2019, Leg bones of a new penguin species from the Waipara Greensand add to the diversity of very large-sized Sphenisciformes in the Paleocene of New Zealand: Alcheringa, v. 44, p. 194–201.
Mayr, G., De Pietri, V.L., Love, L., Mannering, A.A., Bevitt, J.J., and Scofield, R.P., 2020, First complete wing of a stem group sphenisciform from the Paleocene of New Zealand sheds light on the evolution of the penguin flipper: Diversity, v. 12, 46. https://doi.org/10.3390/d12020046.
Miller, J.F., 1778, Icones Animalium et Plantarum: London, Letterpress, 54 pl.
Moore, P.J., Douglas, M.E., Mills, J.A., McKinley, B., Nelson, D., and Murphy, B., 1991, Results of a pilot study (1990–1991): marine-base activities of yellow-eyed penguins: Science and Research Internal Report No. 110, Wellington, New Zealand, Department of Conservation, 53 p.
Morgans, H.E.G., 2009, Late Paleocene to middle Eocene foraminiferal biostratigraphy of the Hampden Beach section, eastern South Island, New Zealand: New Zealand Journal of Geology and Geophysics, v. 52, p. 273–320.
Myrcha, A., Tatur, A., and del Valle, R., 1990, A new species of fossil penguin from Seymour Island, West Antarctica: Alcheringa, v. 14, p. 195–205.
Oliver, W.R.B., 1930, New Zealand Birds: Wellington, New Zealand, Fine Arts (N.Z.), 541 p.:
Pittman, M., Heers, A.M., Serrano, F.J., Field, D.J., Habib, M.B., Dececchi, T.A., Kaye, T.G., and Larsson, H.C.E., 2020, Methods of studying early theropod flight: Bulletin of the American Museum of Natural History, v. 440, p. 277–294.
Pyenson, N.D., and Vermeij, G.J., 2016, The rise of ocean giants: maximum body size in Cenozoic marine mammals as an indicator for productivity in the Pacific and Atlantic oceans: Biology Letters, v. 12, 20160186. https://doi.org/10.1098/rsbl.2016.0186.
Richards, M.D., 2019, Two Giant Penguins from the Eocene–Oligocene of Otago, New Zealand [M.Sc. thesis]: Dunedin, Otago, New Zealand, University of Otago, 237 p.
Riska, B., 1991, Regression models in evolutionary allometry: The American Naturalist, v. 138, p. 283–299.
Sharpe, R.B., 1891, A review of recent attempts to classify birds; an address delivered before the Second International Ornithological Congress on the 18th of May, 1891, *in* Proceedings of the 2nd International Ornithological Congress, Budapest, Taylor and Francis, 90 p.
Simpson, G.G., 1946, Fossil penguins: Bulletin of the American Museum of Natural History, v. 87, p. 7–99.
Simpson, G.G., 1971, A review of the pre-Pliocene penguins of New Zealand: Bulletin of the American Museum of Natural History, v. 144, p. 319–378.
Simpson, G.G., 1972, Pliocene penguins from North Canterbury: Records of the Canterbury Museum, v. 9, p. 159–182.
Simpson, G.G., 1981, Notes on some fossil penguins, including a new genus from Patagonia: Ameghiniana, v. 18, p. 266–272.
Slack, K.E., Jones, C.M., Ando, T., Harrison, G.L., Fordyce, R.E., Arnason, U., and Penny, D., 2006, Early penguin fossils, plus mitochondrial genomes, calibrate avian evolution: Molecular Biology and Evolution, v. 23, p. 1144–1155.
Smith, N.A., 2011, Taxonomic revision and phylogenetic analysis of the flightless Mancallinae (Aves, Pan-Alcidae): ZooKeys, v. 91, p. 1–116.
Stadler, T., 2010, Sampling-through-time in birth-death trees: Journal of Theoretical Biology, v. 267, p. 396–404.
Swofford, D.L., 2003, PAUP*. Phylogenetic Analysis Using Parsimony (* and Other Methods): Sunderland, Sinauer Associates.
Tambussi, C.P., Reguero, M.A., Marenssi, S.A., and Santillana, S.N., 2005, *Crossvalia unienwillia*, a new Spheniscidae (Sphenisciformes, Aves) from the late Paleocene of Antarctica: Geobios, v. 38, p. 667–675.
Thomas, D.B., and Ksepka, D.T., 2016, The Glen Murray fossil penguin from the North Island of New Zealand extends the geographic range of *Kairuku*: Journal of the Royal Society of New Zealand, v. 46, p. 200–213.
Thomas, D.B., Ksepka, D.T., and Fordyce, R.E., 2011, Penguin heat retention structures evolved in a Greenhouse Earth: Biology Letters, v. 7, p. 461–464.
Thomas, D.B., Ksepka, D.T., Holvast, E.J., Tennyson, A.J.D., and Scofield, R.P., 2020a, Re-evaluating New Zealand's endemic Pliocene penguin genus: New Zealand Journal of Geology and Geophysics, v. 63, p. 324–330.

https://doi.org/10.1017/jpa.2022.88 Published online by Cambridge University Press

Thomas, D.B., Tennyson, A.J.D., Scofield, R.P., Heath, T.A., Pett, W., and Ksepka, D.T., 2020b, Ancient crested penguin constrains timing of recruitment into seabird hotspot: Proceedings of the Royal Society B: Biological Sciences, v. 287, 20201497. https://doi.org/10.1098/rspb.2020.1497.

Warheit, K.I., 1992, A review of the fossil seabirds from the Tertiary of the North Pacific—plate-tectonics, paleoceanography, and faunal change: Paleobiology, v. 18, p. 401–424.

Warheit, K.I., and Lindberg, D.R., 1988, Interactions between seabirds and marine mammals through time: interference competition at breeding sites, *in* Burger, J., ed., Seabirds and Other Marine Vertebrates: Competition, Predation, and Other Interactions: New York, Columbia University Press, p. 292–328.

Watanabe, J., Field, D.J., and Matsuoka, H., 2021, Wing musculature reconstruction in extinct flightless auks (*Pinguinus* and *Mancalla*) reveals incomplete convergence with penguins (Spheniscidae) due to differing ancestral states: Integrative Organismal Biology, v. 3, p. obaa040. https://doi.org/10.1093/iob/obaa040.

Watanuki, Y., and Burger, A.E., 1999, Body mass and dive duration in alcids and penguins: Canadian Journal of Zoology, v. 77, p. 1838–1842.

Williams, T.D., 1995, The Penguins: Oxford, Oxford University Press, 295 p.

Accepted: 12 September 2022

https://doi.org/10.1017/jpa.2022.88 Published online by Cambridge University Press